

POLYMERIC COMPOSITES WITH CELLULOSE NANOMATERIALS:  
DEVELOPMENT OF SYNERGISTIC TREATMENTS AND STABILIZATION  
SCHEMA

A Dissertation

by

BLAKE TEIPEL

Submitted to the Office of Graduate and Professional Studies of  
Texas A&M University  
in partial fulfillment of the requirements for the degree of

DOCTOR OF PHILOSOPHY

Chair of Committee,	Mustafa Akbulut
Committee Members,	Terry Creasy
	Micah Green
	Mark Holtzapple
Head of Department,	Ibrahim Karaman

August 2016

Major Subject: Materials Science and Engineering

Copyright 2016 Blake Teipel

## ABSTRACT

A combination of scientific and commercial research efforts are presented in this work. Exploits in both early- and late-stage research and subsequent scale-up opportunities are discussed, in particular, highlighting novel idea-to-market approaches suitable for composite materials with nanoscale fillers. Both polymeric and metallic nanocomposites are commercially explored, whereas answers to fundamental questions for polymeric composites filled with biologically derived nanomaterials are provided.

In the first example, the role of a stabilizer in the stiffening and strengthening of cellulose nanocrystal (CNC) filled epoxy was studied. Cetyltrimethylammonium bromide (CTAB), a cationic surfactant, and Boehmite nanoclay (Boe) were mixed with CNCs in water during processing. Boe+CTAB synergistically stiffened the CNC-epoxy composites, increasing elastic modulus by 72% over neat epoxy and 49% over unstabilized CNC-epoxy composites. Boe-treated CNC-epoxy composites exhibited a 23% increase in tensile strength over unfilled epoxy and a 63% increase over an unstabilized CNC-epoxy composite. These nanocomposites also maintained the strain-at-failure of neat epoxy and increased the storage modulus above  $T_g$  by 96%.

Then, in a second example, amine functionalization provided a functional layer between cellulose nanocrystals (CNCs) and polypropylene. Diethylenetriamine (DETA) was combined with polypropylene (PP) and then with CNCs in high-shear mixing. DETA-treatment stiffened the CNC-PP composites increasing elastic modulus by 75% over neat PP and untreated CNC-PP composites. DETA-treated CNC-PP composites

also exhibited a 32% increase in tensile strength over unfilled PP and a 28% improvement for CNC-PP composites without DETA treatment. These nanocomposites were prepared without the use of organic solvents using a scalable, high-volume manufacturing approach. A commercial scale-up plan for this work is presented in detail.

Thermal interface materials (TIMs) are required to enhance the contact between component surfaces, decrease thermal interfacial resistance, and increase heat conduction across the interface. A new TIM discussed herein is prepared using an already established technique of electrocodeposition, forming a flexible, nanocomposite film. The film is highly compliant, utilizing an ultra-high thermal conductivity greater than 250 W/m·K, as opposed to the best commercially available TIMs with conductivities ranging from 5–80 W/mK. This technology also achieves a total bulk thermal impedance of  $1-4 \times 10^{-3}$  K·cm<sup>2</sup>/W, an order of magnitude lower than commercially available TIMs.

## DEDICATION

I dedicate this work to my family including primarily my wife, Elisa, our first child Olive Rosemary, who went to Heaven May 12, 2015, our second child Oak Blake, our future children and our other family.

## ACKNOWLEDGEMENTS

I would like to thank my committee chair, Dr. Akbulut, and my committee members, Dr. Creasy, Dr. Green, and Dr. Holtzapple, for their guidance and support throughout the course of this research.

Thanks also to my friends and colleagues in the Materials Science and Engineering and the Department Chemical Engineering faculty and staff for making my time at Texas A&M University a great experience. A hearty thank you is extended to my friends at Mays Business School who have enlivened my academic tenure tremendously. I also wish to extend my gratitude to the National Science Foundation, whose helpful funding under the Small Business Innovation Research Grant program enabled some early work and continues to fund future work as discussed in Chapter IV. Also, a special thank you to Elizabeth Johnston-Tengler and Chuck Rocco at Ford Motor Company who provided industrially sourced funding and helpful voice-of-the-customer input throughout the early stages of the research and commercialization process. I would also like to acknowledge my colleagues at Essentium Materials, LLC for funding much of this work and helping with larger batch processing: Elisa Guzman-Teipel, Ph.D., Ryan Vano, Bryan Zahner and Matt Kirby (former). A special thank you to Mr. Gene Birdwell, co-founder of Essentium Materials, without whose unwavering support and financial backing of the research team, none of this work would have been possible. I also wish to thank Will Seward and Ron Smith for their expert mold machining; Dr. Robert Taylor and Debbie Perry for use of their freeze-driers. I also acknowledge Texas

A&M University's Materials Characterization Facility and Microscopy Imaging Center for training and electron microscopy imaging assistance. And way back in the beginning, I thank Dr. Alan Rudie at the USDA Forest Products Lab for his helpful conversations.

Finally, a very deep thank you to my dear wife for her patience and love, and my mother, father, brother and sister-in-law, for their consistent encouragement. Also, I extend my thanks to my mother-in-law, father-in-law and sister-in-law for their practical help and constant support.

## NOMENCLATURE

CN(s)	Cellulose nanomaterial(s)
NC	Nanocellulose
CNC(s)	Cellulose nanocrystal(s)
CNC-L(s)	Lignin-coated Cellulose nanocrystal(s)
CNF(s)	Cellulose nanofibril(s)
CTAB	Cetyltrimethylammonium bromide
Boe	Boehmite
DETA	Diethylenetriamine
PP	Polypropylene
PA	Polyamide
MAH	Maleic acid group
MAPP	Maleated Anhydride Polypropylene
MA	MAPP-Amine
Boe	Boehmite
HVM	High volume manufacturing
IM	Injection molding
GDC	GDC Corporation
SWTR	Strength to weight ratio
RWP	RWP Kinsale Corporation
GM	General Motors Corporation

TIM(s)	Thermal Interface Material(s)
IP	Instrument panel
API	American Process Incorporated
SAM	Served Available Market
CAGR	Combined Annual Growth Rate
USD	United States Dollar
VC	Venture Capital(ist)
OEM	Original Equipment Manufacturer
BN	Boron Nitride
BNNS	Boron Nitride Nanosheet
TRL	Technology Readiness Level
MRL	Manufacturing Readiness Level
VoM	Voice of the Market
NSF	National Science Foundation
TAMU	Texas A&M University
SBIR	Small Business Innovation Research (program)
FTE	Full Time Equivalent
T <sub>g</sub>	Glass Transition Temperature



## TABLE OF CONTENTS

	Page
ABSTRACT.....	ii
DEDICATION.....	iv
ACKNOWLEDGEMENTS.....	v
NOMENCLATURE.....	vii
TABLE OF CONTENTS.....	ix
LIST OF FIGURES.....	xi
LIST OF TABLES.....	xiv
CHAPTER I INTRODUCTION AND LITERATURE REVIEW.....	1
On the approaches in this work.....	7
CHAPTER II CELLULOSE NANOCRYSTALS AND BOEHMITE NANOCCLAY IN EPOXY COMPOSITES.....	8
Experimental.....	9
Results and discussion.....	12
CHAPTER III CELLULOSE NANOCRYSTALS IN POLYPROPYLENE COMPOSITES.....	21
Experimental.....	22
Results and discussion.....	26
CHAPTER IV CELLULOSE NANOMATERIALS IN THE MARKETPLACE.....	36
Potential uses for composites with CNs.....	38
Scale up plans.....	39
Cost analysis: Raw material supply and pricing.....	39
Competing technologies.....	40
“Valley of Death” commercialization plan.....	41
Customer analysis.....	42
Industry overview & customers.....	45
Market analysis.....	46

Intellectual property landscape .....	51
Finance & revenue model .....	53
Model for projecting revenues for 3 years post Phase II .....	56
<b>CHAPTER V CONCLUSIONS .....</b>	<b>58</b>
On the general approach .....	58
CNC-boehmite .....	60
CNC-PP.....	61
Commercial scale up efforts to date.....	62
Broader impact.....	62
Summary from Appendix: Thermal interface materials .....	63
On the author's professional philosophy .....	63
<b>REFERENCES .....</b>	<b>65</b>
<b>APPENDIX: COMMERCIALIZATION OF NEXT-GENERATION NANOCOMPOSITES. CASE STUDY OF METAL-MATRIX THERMAL INTERFACE MATERIALS.....</b>	<b>78</b>
Description of the problem .....	78
Description of the proposed solution .....	81
Development plan .....	87
Description of the potential commercial impact.....	99
Results from the National Science Foundation I-Corps program.....	99
Conclusions: Thermal Interface Materials.....	102

## LIST OF FIGURES

	Page
Figure 1: Cellulose nanocrystals imaged by atomic force microscopy (AFM).....	3
Figure 2: Energy consumed in the preparation of various fillers, polymeric resins, and metals. ....	5
Figure 3: Scanning electron micrographs of unstabilized CNCs (a), Boehmite clay (b), CTAB-stabilized CNCs (c) Boehmite-stabilized CNCs (d), CNC:Boe (e), and Boehmite-only microsphere (f) in epoxy. All composites contain 10 wt% of a given filler. ....	13
Figure 4: Tensile stress as a function of strain for neat epoxy, CTAB-stabilized CNCs, Boehmite only and Boe-stabilized CNCs. All composites contain 10 wt% of a given filler system.....	15
Figure 5: Schematic of nanocrystals (a), clay-coated nanocrystals (b), and behavior in the presence of crack-growth (CNC:Boehmite in upper crack and CNC-only in lower crack) (c). ....	16
Figure 6: Tensile modulus (a), strength (b) and strain at break (c) as a function of solids concentration in epoxy.....	18
Figure 7: Storage (a) and loss modulus (b) as a function of temperature for epoxy-based composites. ....	20
Figure 8: Schematic representation of two-step DETA-MA-CNC functionalization: neat MAPP (a) melt-mixed with DETA (b) creating DETA-functionalized MAPP (and water) (c); DETA:MA (d) added to CNCs (e) which forms a polymer-coated CNC, f). ....	24
Figure 9: Infrared spectroscopy of the DETA-MAPP-CNC functionalization; the effect of the MAH:NH <sub>2</sub> ratio (a) and the effect of increasing CNC:MA concentration (b). The 1:1 MAH:NH <sub>2</sub> composite in (a) mixed at 1:10 CNC:MA; samples for data in (b) loaded at 5 wt% CNC.....	28
Figure 10: Tensile stress (MPa) vs tensile strain (mm/mm) for DETA-MA-CNC composites showing the effect of MAH:NH <sub>2</sub> ratio (a) and the effect of increasing MA particle coverage (b). ....	31
Figure 11: Summary of mechanical properties as a function of CNC loading (wt%) (a) and (b); the effect of individual components of the chemistry (c) and (d).	

Error bars represent $\pm$ one standard deviation, based on at least five measured specimens for each composition. ....	33
Figure 12: Composite microstructure as a function of CNC and DETA-MA-CNC treatment. Neat PP (a); PP with untreated CNCs (b); PP microstructure with 1:5 CNC:MA (c); PP microstructure with 1:10 CNC:MA (d). ....	35
Figure 13: Investment money as a function of an invention's position in the overall innovation process (a). Major funding sources, research stage and overall position of the CN-polymer composites in this work (b). ....	37
Figure 14: Instrument panel – target automotive part. ....	44
Figure 15: Value chain for structural automotive interior parts. ....	45
Figure 16: US Market segmentation for nanocomposites (2013). <sup>84</sup> ....	49
Figure 17: Search for fundamental understanding vs Consideration for use. <sup>94</sup> ....	64
Figure 18: Heat generation occurs in microelectronic and semiconductor devices and can lead to device inoperation and failure. ....	78
Figure 19: Users of all types of devices are hindered when thermal mis-management causes device shut down. ....	79
Figure 20: Surface mismatch between thermal source and heat sink (Atomic Force Microscopy (AFM) surface contour shown). ....	81
Figure 21: Poor surface-surface contact leads to poor thermal conductivity. ....	82
Figure 22: Next generation Thermal Interface Materials. ....	83
Figure 23: Current Generation Thermal Interface Materials with corresponding thermal conductivities. ....	84
Figure 24: Three step process to produce next-generation TIMs. ....	85
Figure 25: Breakthrough TIMs must exhibit low elastic modulus and high thermal conductivity. ....	86
Figure 26: Innovation stage: Next generation Thermal Interface Materials. ....	87
Figure 27: The National Science Foundation I-Corps Program mandates customer discovery away from users who may be familiar with a technology under investigation. ....	94

Figure 28: Typical customer archetype, a typical customer constraint (Moore’s Law) and example end-use applications for TIMs. ....	95
Figure 29: TIMs Development Timeline and Milestones.....	98
Figure 30: End-user feedback was gained from technical groups across the United States. ....	101
Figure 31: Feedback from selected End Users. ....	102

## LIST OF TABLES

	Page
Table 1 - Stabilization Ratio Determined via DLS .....	10
Table 2 - Raw Materials Cost Summary at Current and Projected Phase II Formulations.....	40
Table 3 - Competitive Summary Table - Automotive Structural Materials .....	41
Table 4 - Current Technologies Being Used and Their Shortcomings .....	43
Table 5 - Milestones Summary Table.....	53
Table 6 - Technology Readiness Level Pertinent Position (selection from full DoD TRL) .....	90
Table 7 - Manufacturing Readiness Level with TIMs position highlighted (selection from full DoD MRL).....	92

## CHAPTER I

### INTRODUCTION AND LITERATURE REVIEW

This effort merges technical contributions in the area of polymer composites with commercial pursuits of the same.

Generally, nanoparticles, both organic and inorganic, offer great promise for a multitude of applications.<sup>1,2</sup> In some instances, hybrid blending of organic and inorganic nanoparticles such as cellulose and silver have shown improved mechanical properties that are complementary.<sup>3</sup> Characteristics such as a high surface-area-to-volume ratio, excellent purity, low density, good mechanical and/or transport properties normally accompany materials on this size scale. Nanoscale fillers are often used to improve functionality of polymer composites, principle examples being nanoclay,<sup>4-6</sup> carbon such as tubes<sup>7,8</sup> and two-dimensional nanomaterials<sup>9,10</sup> and polysaccharide materials (e.g., CNs).<sup>11,12</sup> At particles with size on the true nanoscale, Brownian motion and surface interactions dominate such that significant effort must be made to influence particle behavior and to obtain particle assemblies which positively influence material properties.<sup>13</sup> Despite this promise, challenges such as dispersion,<sup>14</sup> interfacial adhesion,<sup>15</sup> and bio-compatibility<sup>16</sup> are present when nanoparticles are introduced into larger-scale systems. To cope with these challenges, nanoparticles must be engineered at their surface to increase compatibility with their carrier (e.g., matrix if a nanocomposite application). Polymer chains are often deployed to the surface, where they are either adsorbed electrostatically (physisorption) or tethered to the surface covalently.<sup>17</sup> These polymer chains can be referred to as polymer brushes and are

applied to both organic and inorganic nanoparticles,<sup>1,18-20</sup> for use both in nanocomposite<sup>21-24</sup> and stimuli-responsive<sup>25-27</sup> applications. For macroscale composite materials to experience the significant mechanical improvements which are theoretically possible by the inclusion of highly stiff and strong nanoparticles, homogeneously dispersed nanoparticles are required. For example, amphiphilic block copolymer nanocomposites demonstrate good dispersions, and rely primarily on self-assembled micelles.<sup>28,29</sup> These micelles can nanocavitate in the presence of shear-strain which improves the strength and crack-growth resistance of macroscale bulk composites.<sup>30</sup> Electrostatic adsorption is another common mechanism by which dissimilar nanoparticles can form stable dispersions; for example, adsorption of nanoclay to carbon nanotubes has provided improved dispersion and subsequent macro-mechanical properties for epoxy composites.<sup>31</sup>

Cellulosic nanomaterials (CNs), are derived from cellulose, the most abundant biopolymer on earth.<sup>14,15,32,33</sup> CNs are excellent candidates for reinforcement of polymers because of their superb tensile strength and elastic modulus, exceeding that of carbon fiber.<sup>14</sup> Cellulose-filled nanocomposites are potentially useful for automotive components,<sup>34</sup> building construction products,<sup>35</sup> and consumer goods.<sup>15</sup> Cellulose nanocrystals (CNCs) are the highly ordered nano-scale crystals (sometimes called nanowhiskers)<sup>33,36</sup> that remain once the amorphous regions are removed from nanofibrils, typically via acid hydrolysis.<sup>14,37</sup> CNCs derived from woody-derived biomass are low density (1.6 g/cm<sup>3</sup>), highly crystalline (54–88%),<sup>14</sup> and roughly rectangular with a moderate aspect ratio (typically 3–5 nm wide, 100-300 nm long).<sup>38</sup>



The present work utilizes CNCs of similar size and aspect ratio as determined by atomic force microscopy (AFM) (Figure 1).

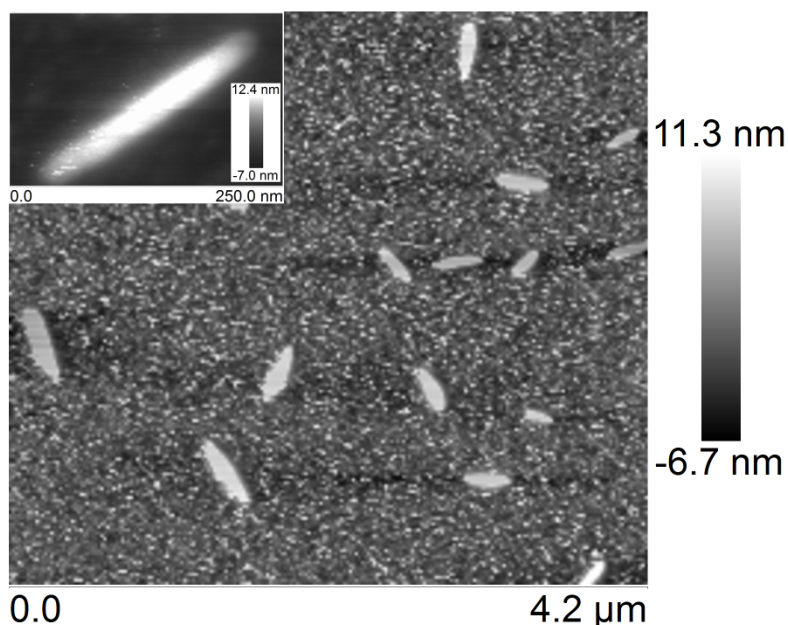


Figure 1: Cellulose nanocrystals imaged by atomic force microscopy (AFM).

Often processed from Kraft pulp sourced from paper mill waste, CNCs are the fundamental building blocks of trees, grasses, and tunicates. Some work has investigated efficient methods to harvest directly from trees and biomass sources.<sup>39</sup> Given their intrinsic hydrophilicity, a significant challenge facing CNC-reinforced polymer composites is interfacial adhesion between the cellulose particle and a polymer matrix.<sup>14,15</sup> Achieving homogeneous CNC dispersion throughout the matrix is a related issue.<sup>14</sup> When considering cost- and sustainability-motivations, cellulose nanocrystals are becoming known as energy-efficient and cost-effective with respect to the complexity of preparation of competitive fillers (e.g., carbon fibers or nanotubes, and

glass fibers). Cellulose nanomaterials and conventional glass fibers require low amounts of energy to produce, at just over 20<sup>40</sup> and 48 MJ/kg,<sup>41</sup> respectively. However, the stiffness and strength of glass fibers (86 and 4.6 GPa, respectively, for S-glass; 70 and 2.8 GPa for E-glass)<sup>42</sup> cannot compete with CNCs or carbon fibers.<sup>14,42</sup> Stiffness and strength values for crystalline cellulose are typically 155 and 7.6 GPa, respectively.<sup>14</sup> In part, because of their high crystallinity, CNCs are virtually defect-free compared to macro-cellulose materials (e.g., wood flours or wood-composite components).<sup>38</sup> Chemically, acid-dissolved nanocrystals are left with a strong negative surface charge of  $-45 \pm 1.8$  mV because of residual sulfate esters that remain as a product of the sulfuric acid treatment.<sup>5</sup> De-protonation at neutral pH is responsible for the high surface charge, resulting in stable aqueous suspensions at loadings > 8 wt%.

Cellulose nanocrystals are regarded as energy-efficient and cost-effective with respect to the complexity of preparation relative to competitive fillers. Figure 2 shows the relative amount of energy required to prepare common fillers, matrix materials and metals.

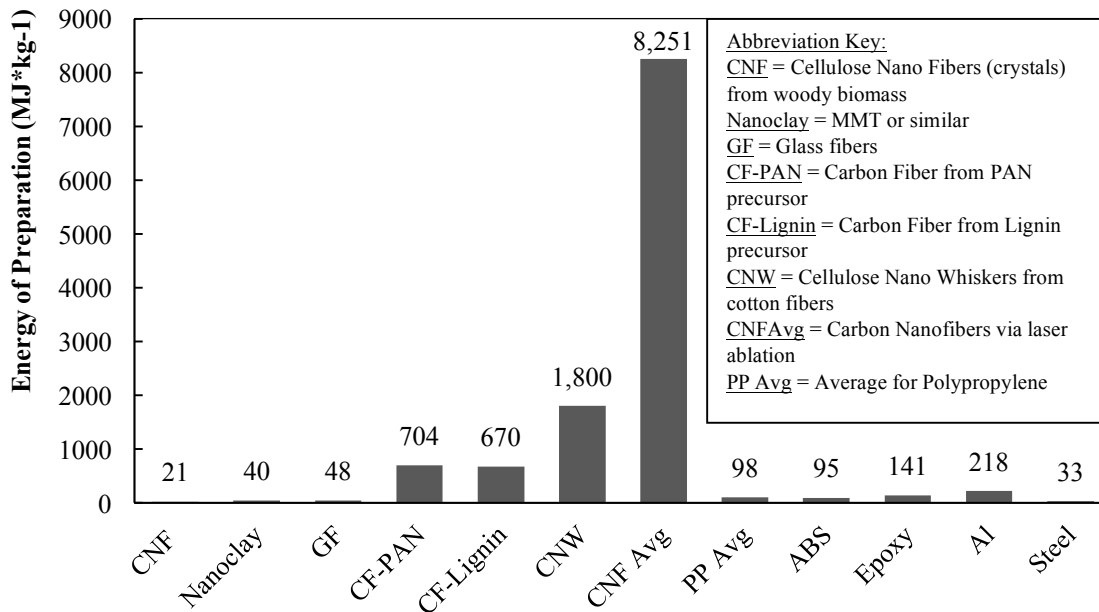


Figure 2: Energy consumed in the preparation of various fillers, polymeric resins, and metals.

At just over 48 MJ/kg, conventional glass fibers are among the most energy-efficient reinforcement.<sup>41</sup> Some nanoclays are also energy-competitive (at 40 MJ/kg)<sup>43</sup> and typically possess platelet structures that impart favorable mechanical properties. Some cellulose nanomaterials can be produced at just over 20 MJ/kg,<sup>40</sup> which is the lowest energy of preparation of any known nano or conventional filler. This low value is for woody biomass taken from raw feedstock that is logged, chipped, wet-cut milled, treated with hot-compressed water, then wet-disk milled (multiple passes).<sup>40</sup> The cellulose nanofibers reported are 15–20 nm in diameter.

Carbon fiber requires between 670–704 MJ/kg to prepare (from two different precursor materials, lignin, and polyacrylonitrile),<sup>44</sup> cellulose nanowhiskers hydrolyzed

from cotton fibers require 1800 MJ/kg,<sup>43</sup> and carbon nanotubes prepared via laser ablation require 8251 MJ/kg.<sup>45</sup> Conventional matrix materials, to which these fillers are added, are also reported for comparison in Figure 2. Polypropylene requires 97.8 MJ/kg,<sup>40,41,45</sup> whereas ABS and epoxy require 95.02 and 140.7 MJ/kg, respectively.<sup>41</sup> Aluminum and steel are also shown for comparison because they sometimes compete with polymer composites in structural applications.<sup>44,45</sup>

Thermoplastics and thermoplastic composites are used widely in myriad of global markets.<sup>46,47</sup> Polyolefins form an especially robust segment of this industry, comprising greater than 50% of the global thermoplastics market – itself a \$109.3 bn market in the U.S.<sup>46,47</sup> An increased focus on improving sustainability,<sup>48</sup> as well as persistent economic pressures drive the need for continuous innovation in this space.<sup>49,50</sup> In addition to low material costs, highly automated processing equipment contributes to low cycle-times and labor requirements in the presence of a mature, global supplier base.<sup>46,47</sup> Additionally, there are readily available mix-in technologies such as compatibilizers designed to enhance interfacial strength between various fillers and polymeric resins,<sup>51</sup> and additives which improve filler dispersion.<sup>52</sup> These have all contributed to propagate thermoplastic composites into applications with increasingly demanding specifications.

Stabilizers such as polymer brushes, surfactants or other molecules are often used to overcome the tendency of CNs to agglomerate (because of attractive Van der Waals forces) in low-polarity media such as polyolefin resins. Coating of the particle or fibril surface by polymer chains can provide either a layer or a brush, depending on the

degree of polymer-chain-to-particle-surface conformation,<sup>17,53</sup> improving strength and bonding at the particle-matrix interface. For example, polyethylene glycol (PEG) has been grafted to the surface of cellulose nanofibrils.<sup>54</sup> Electrostatic adsorption of a cationic surfactant, such as cetyltrimethylammonium bromide (CTAB), to the surface of CNCs has shown promise stabilizing dispersions in apolar solvents.<sup>55</sup> Stabilization via polyethylene oxide (PEO) has also been reported to stabilize nanoparticles in solvent,<sup>33</sup> along with variety of other molecules, polymers, and clays.<sup>56-58</sup>

*On the approaches in this work*

The bulk of the prior work in the field has been focused on improving the dispersion quality of CNs in a variety of media. Although beneficial from an empirical and traditional standpoint, this common approach has left an opportunity to focus on preparation methods of nanocomposites with CNs incorporated, that are prepared using (1) environmentally friendly and (2) cost-effective schema. The cellulose community will be well-served from applications of CNs that break previous cost barriers by competing with commodity plastic resins economically, and which are available for preparation in high-volume manufacturing (HVM) approaches.

This work has therefore explored the quickest pathways to integrate cellulose nanomaterials into the marketplace and to do so by targeting commercial applications that hold promise for broad adoption from a variety of down-stream manufacturing practices, principle among which is injection molding (IM). A secondary focus of this work was to explore the ability of CNs to strengthen epoxy composites with promising commercial applications in areas such as bulk composites, adhesives, and thin films.

## CHAPTER II

### CELLULOSE NANOCRYSTALS AND BOEHMITE NANOCCLAY IN EPOXY COMPOSITES\*

In the first study performed under the context of this broader work, cationic nanoclay and a common surfactant were used to stabilize cellulose nanocrystals in epoxy. Nanoclay appeared to create physical interlocks at the epoxy-nanoclay interface, increasing the tensile strength and promoting overall crack resistance through the composite. The epoxy resin and anhydride hardener system used here were selected to provide shorter, elevated-temperature cure times. Epoxy systems with amine hardeners have been previously investigated with CNCs, but cure times have been in excess of 12 hours.<sup>59,60</sup> The approach taken in this work reduced the cure time to 4 hours and eliminated the use of organic solvent by combining the stabilized CNCs directly into the resin and utilizing lyophilization for water removal. CNCs stabilized with nanoclay were shown to improve stiffness, strength and thermal stability, whereas maintaining elongation of this epoxy system. The synergy of the CNC:nanoclay system is primarily because of increased mechanical interface between the polymer and the filler. With clay acting as a green stabilizer for CNCs, this unique combination is very promising for improving epoxy thermomechanical behavior and reducing the environmental footprint of these nanocomposites.

---

\* Reprinted with permission from [Synergy in epoxy nanocomposites with cellulose nanocrystals and Boehmite](#): Blake R. Teipel and Jaime Grunlan, Green Materials 2014 2:4, 222-231

## *Experimental*

### **Materials**

Cellulose nanocrystals were purchased from the Forest Products Laboratory (Madison, WI) as a 7.2 wt% aqueous suspension. CTAB was purchased from Sigma Aldrich (Milwaukee, WI) and used as received. Boehmite (Boe) nanoplatelets were provided by Esprix Technologies (Sarasota, FL) and used as received. A diglycidol-ether of bisphenol-A epoxy resin (D.E.R 383), with epoxide equivalent weight of 176–183 g/eq, was provided by the Dow Chemical Company (Midland, MI). Anhydride hardener (LS-81K) was provided by Lindau Chemicals (Columbia, SC). Both epoxy components were used as received.

### **Nanocomposite preparation**

Varying amounts of CTAB, Boe and CTAB+Boe were added to 20-mL aqueous suspensions containing 0.1 wt% CNC. A Malvern Instruments (Westborough, MA) Zetasizer Nano ZS90 was used to measure the zeta potential of the various mixtures. This technique was used to determine the amount of stabilizer required to achieve (or move toward) charge neutrality. The Boehmite and CTAB+Boehmite stabilization ratios were also determined this way. Table 1 summarizes the minimum stabilizer ratio possible to achieve charge neutrality, which is reflected as a near-zero zeta potential ( $\zeta$ ). Although the CNC:Boe ratio shown in Table 1 did not achieve complete charge neutrality, it effectively stabilized the CNCs and improved mechanical properties of the composites.

Table 1 - Stabilization Ratio Determined via DLS

Recipe	Mass Ratio	$\zeta$ Avg (mV)	$\zeta$ Std Dev (mV)
Aqueous CNC	-	-37	8.2
Aqueous CTAB	-	+61	14
Aqueous Boe	-	+40	9.8
CNC:CTAB	8:1	-1.5	4.2
CNC:CTAB:Boe	8:1:1	-10	4.1
CNC:Boe	1:4	-19	4.8

After addition of the stabilizer to the aqueous CNC suspension, unbound stabilizer was removed with three cycles of centrifugation, rinsing, and redispersion. Centrifugation was performed on 45-mL samples at 2500 rpm for 15 minutes. The supernatant was then discarded, precipitated nanoparticles retained and fresh DI water was added (filling the vials again to 45 mL). Redispersion was performed by stirring the mixture in the vials with an overhead mixer at 550 rpm, resulting in a uniform solution in 2–3 mins. After three cycles, the supernatant zeta potential was measured to ensure the supernatant was charge-neutral, indicating removal of all unbound stabilizer. The stabilized CNCs were then freeze-dried after mixing with 9 vol% *t*-butyl alcohol (to resist ice-crystal formation) in a tray-type freeze dryer for 96 hours. The resulting dried cake was pulverized via roller-milling for between 1 and 8 hours. Unstabilized CNCs



were also freeze-dried from aqueous suspension and roller-milled for 8 hours to achieve an appropriate powder consistency. A dried cake of stabilized CNCs only required between 1 and 2 hours to achieve this consistency.

The resulting stabilized CNC powders were added directly to D.E.R. 383 resin in a 100 mL glass beaker and stirred with a spatula at 85°C for 5 minutes. The mixture was tip-sonicated at 26W for 3–5 minutes with stirring. Hardener:resin was then added at a 0.87:1.0 ratio and the system was spatula-stirred for an additional 5 minutes. The system was degassed in a vacuum oven for 20 minutes at 85°C before being poured into an aluminum mold containing milled cavities of various ASTM test-specimen geometries. This mixture was cured for two hours at 85°C, followed by two hours at 185°C. Five samples of each recipe were analyzed for statistical purposes. Composites were filled with 2, 4, and 10 wt% (total solids) nanoparticles. When CTAB was used its weight was neglected so the total filler content refers only to the percentage of CNCs, Boehmite or CNC+Boehmite. The CNC loading was only 25 wt% of the total for the CNC:Boehmite composites. Boehmite-only composites were made with 2, 4, and 10 wt% in order to compare to the CNC:Boehmite mixture. For the composites containing CTAB, there was excess surfactant present in the solution (prior to centrifugation-rinse). The critical micelle concentration (CMC) of CTAB is above 0.05 M,<sup>32,61</sup> but three cycles of centrifugation, rinse, and re-dispersion were successful in removing the unbound surfactant. The lack of bubbles in the final composites, combined with the reduction of foam from the supernatant after the first and second centrifugation, suggests that the majority of excess CTAB was removed.

## *Results and discussion*

### **Composite microstructure**

Figure 3 shows micrographs of the fracture surfaces of tensile-test specimens. In the composite containing untreated CNCs, several crystals can be seen in the fracture surface (Figure 3(a)). It appears that the failure mode was particle-pull out, with the shape and morphology of the individual crystals matching that reported elsewhere.<sup>14,38</sup> Figure 3(b) shows Boehmite in epoxy, with both epoxy-only and Boehmite-rich regions visible. Epoxy has a glassy appearance, whereas the Boehmite-rich areas have a granular look. The composite containing CTAB-stabilized CNCs seems to have failed at the epoxy-CTAB interface rather than the CTAB-CNC interface (Figure 3(c)). Evidence for this is observed in the coarse morphology shown in the Figure 3(c) inset. Strong electrostatic interactions are reported between CTAB and CNCs,<sup>55</sup> which supports this assumption.

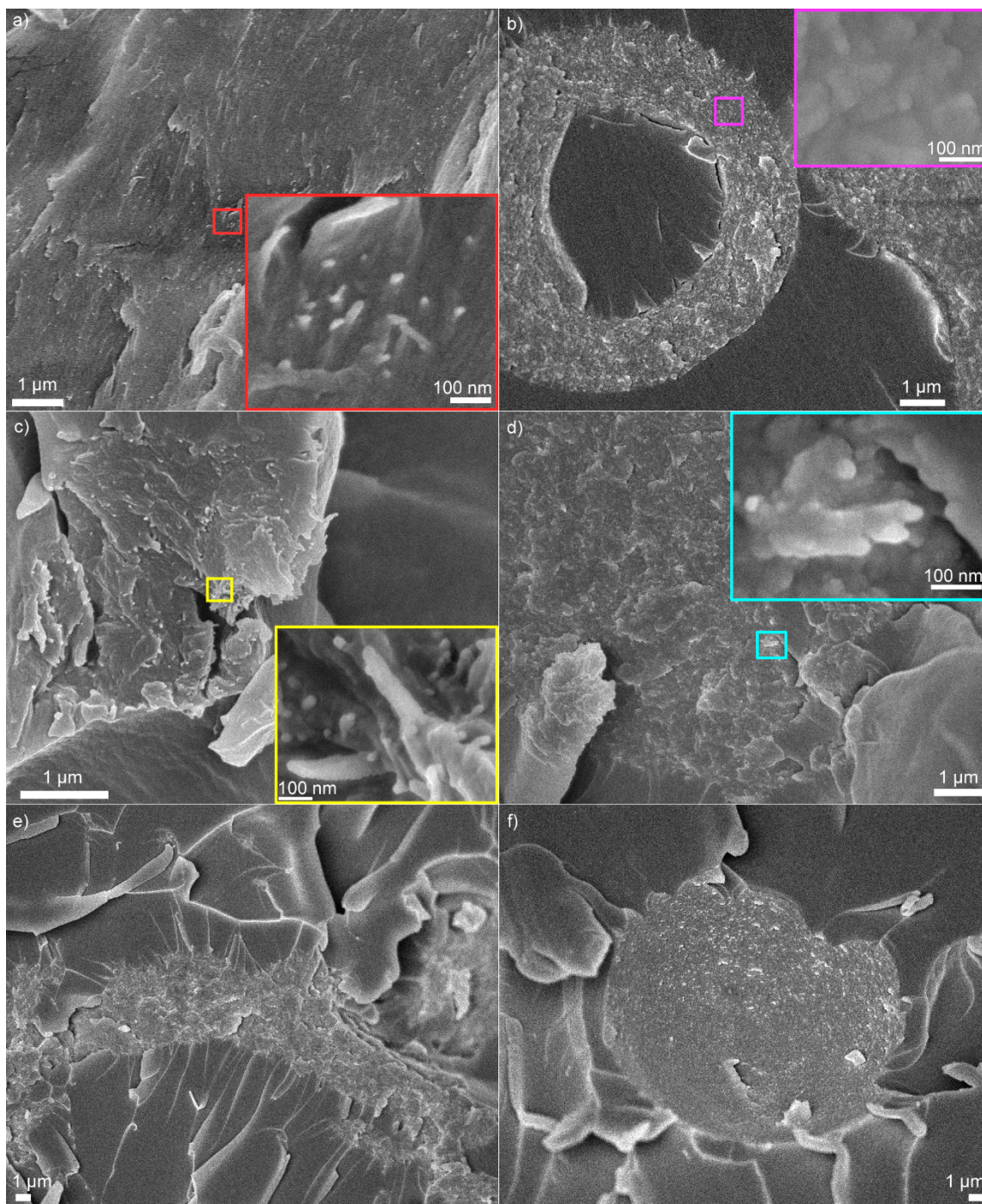


Figure 3: Scanning electron micrographs of unstabilized CNCs (a), Boehmite clay (b), CTAB-stabilized CNCs (c) Boehmite-stabilized CNCs (d), CNC:Boe (e), and Boehmite-only microsphere (f) in epoxy. All composites contain 10 wt% of a given filler.

Interestingly, the Boehmite in the Boehmite-only composites formed occasional spherical and microcapsule-like agglomerates in multiple places (Figure 3(b), (e) and (f)). A possible explanation for this tendency to self-assemble is that in an effort to minimize surface area in contact with the hydrophobic resin, the hydrophilic nanoclay forms these thermodynamically favorable structures. There are several examples of pickering emulsions of nanoclay and colloidal silica within apolar epoxy.<sup>19,62-64</sup> This surface-energy-driven interfacial phenomenon could explain the tendency of the Boe to spread into bands, to increase surface area:volume ratio, as the presence of CNCs moves the mixture towards charge-neutrality within the resin.

### **Composite mechanical behavior**

Five samples of each recipe were analyzed via tensile testing according to ASTM D638. Figure 4 shows stress-strain plots for selected specimens containing 10 wt% nanoparticles (surfactant weight is neglected; the total filler content refers to the percentage of CNCs, Boehmite or CNC+Boehmite where applicable). The 1:4 loading of CNC:Boe increases stiffness 56% over neat epoxy and 35% over unstabilized CNCs. There is significant synergy between the cellulose nanocrystals and the Boehmite. The CNC:Boe composites are significantly stronger than composites containing only Boehmite. Composites loaded with an 8:1:1 ratio of CNC:CTAB:Boehmite had 72% higher stiffness than neat epoxy and 49% over unstabilized CNCs, but the strength and elongation were diminished (relative to neat epoxy). This behavior is likely caused by insufficient clay present to sufficiently coat the surface of the CNCs and form a roughened surface to which the polymer can more effectively cling. The CTAB

modestly aids the dispersion of the CNCs, which improves the stiffness of the composite by creating an increased percolative-stress network. Tensile strength of the composite is diminished, however, because of the lack of a good physical-interlock between the epoxy and the nanocrystal, created in and around a strongly bound nanoparticle-nanocrystal system (e.g., the CNC:Boe system).

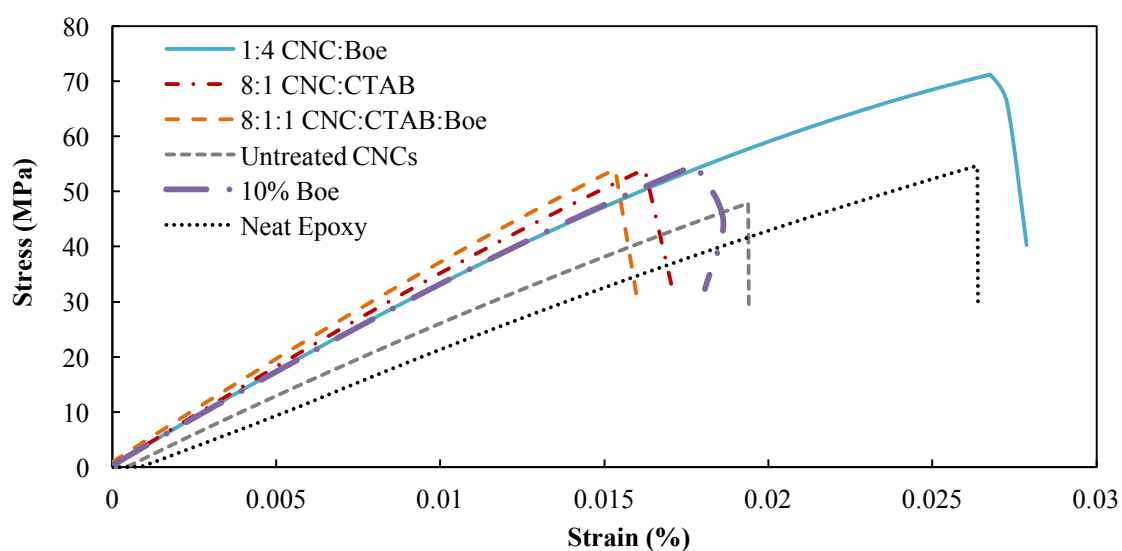


Figure 4: Tensile stress as a function of strain for neat epoxy, CTAB-stabilized CNCs, Boehmite only and Boe-stabilized CNCs. All composites contain 10 wt% of a given filler system.

Figure 5 schematically illustrates a possible explanation for the increased strength observed for the 1:4 CNC:Boehmite-filled composites. CNCs have a relatively smooth surface in the absence of clay (Figure 5 (a)). With the addition of clay, a significantly rougher surface is produced because of electrostatic adsorption (Figure 5 (b)). The primary mechanism for increased strength and the maintenance of elongation

under load is mechanical in nature. Figure 5 (c) illustrates that with clay adsorbed to the surface of the CNC (upper crack), the epoxy has a physical interlock that prevents crack widening. Particle pullout and unhindered crack propagation occur without this physical interlock mechanism (lower crack). This pullout was observed experimentally in Figure 3(a).

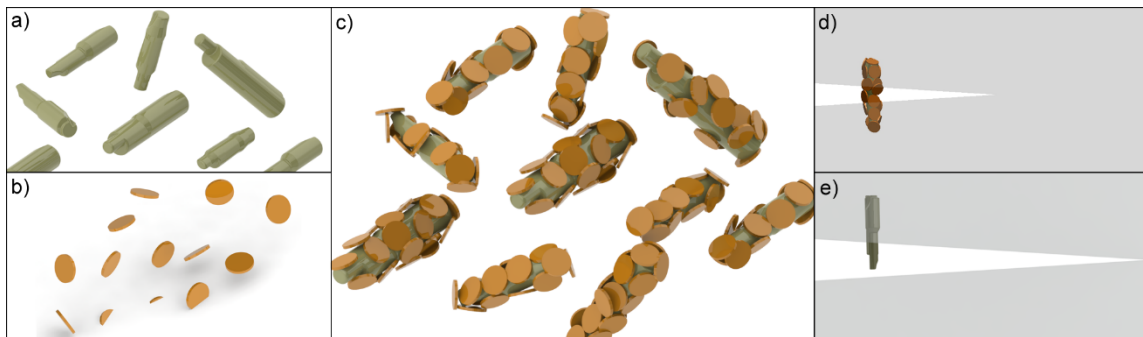


Figure 5: Schematic of nanocrystals (a), clay-coated nanocrystals (b), and behavior in the presence of crack-growth (CNC:Boehmite in upper crack and CNC-only in lower crack) (c).

Figure 6 shows modulus, strength and elongation for all composite systems studies here. Error bars represent  $\pm$  one standard deviation, based on five measured specimens for each composition. As expected, modulus increases with solids concentration (Figure 6 (a)), with the exception of CNC:Boe at 10 wt%. Composites of this type had a slightly diminished stiffness at the higher loading (e.g., -1.4%), down from 3477 to 3428 MPa compared to 4 wt%. There are filler loadings within epoxy composites beyond which there is no mechanical gain, where the saturation limit is reached and aggregation occurs.<sup>60</sup> When agglomerated, nano-scale fillers approach the

micron-scale allowing easier crack propagation and decreased fracture toughness.<sup>60</sup> The average strength decreases for every composite, as compared to neat, except for the 1:4 CNC:Boe, for which the strength increases 23% from 61 to 75 MPa. This composite increases the strength of the composite filled with untreated CNCs by 63%. Strain at break was maintained at 3.0% for the 1:4 CNC:Boe composite as compared to neat, and notably the standard deviation decreased 50% to  $\pm 0.21\%$ , and decreased 55% from composites loaded at 2 wt% Boehmite. Overall the standard deviations for modulus, strength and strain at break for the 1:4 CNC:Boe are the smallest for any of the composites tested in this work.

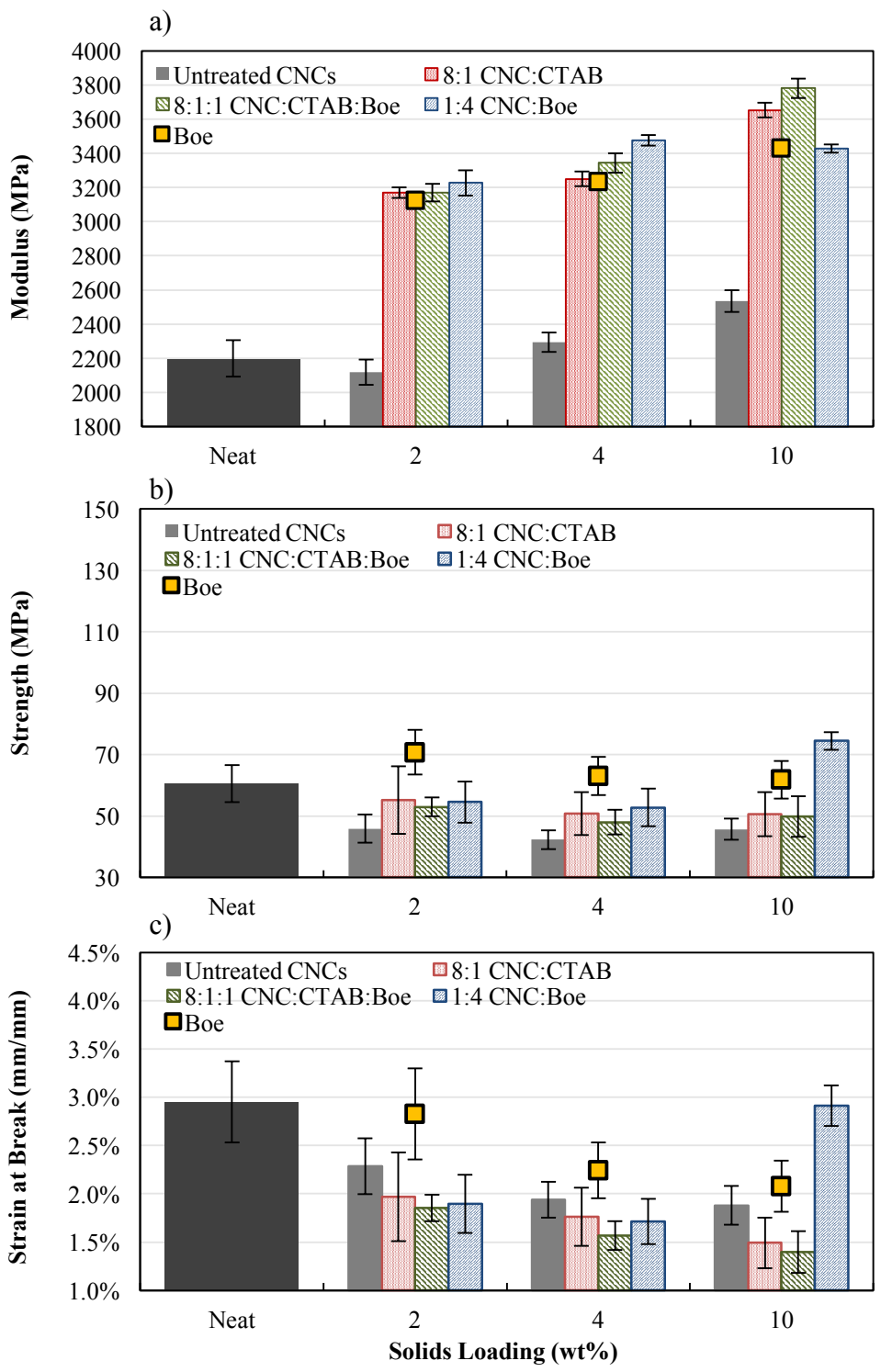


Figure 6: Tensile modulus (a), strength (b) and strain at break (c) as a function of solids concentration in epoxy.



## Composite thermal behavior

Dynamic tensile testing was conducted on three specimens of each composite recipe at 10% loading, (Figure 7). The average storage modulus for the epoxy composites shows that the presence of CNCs does not impart significant mechanical improvement over neat epoxy below  $T_g$ . This is commonly observed for CNC-loaded composites in their glassy state.<sup>57,65,66</sup> The loss modulus did not change with the presence of CTAB-stabilized CNCs (i.e., there was no noticeable increase in  $T_g$ ) or Boehmite. The composite containing 1:4 CNC:Boe showed a 6.3% increase in  $T_g$  over neat epoxy, rising to 152°C. Above  $T_g$ , the storage modulus of this composite improved by 96%, rising from 19 to 38 MPa. The 8:1:1 CNC:CTAB:Boe improved the storage modulus by 110% to 41 MPa. It is believed that the dispersion of the epoxy was improved by the presence of the CTAB, although the CTAB itself degraded above 165°C. The 8:1 CNC:CTAB composite showed the same initial storage modulus improvement that the CTAB:Boe recipe did, but quickly fell off above 168°C. Nanoclay has been shown to thermally shield polymer nanocomposites in other work,<sup>4</sup> making this a likely mechanism for the improved response of the 8:1:1 CNC:CTAB:Boe over the composites with no Boehmite. Nanoclay is additionally thought to prevent intra-gallery interdiffusion of polymers,<sup>67</sup> which contributes to a protective layer over the CNC (in the 1:4 CNC:Boe specimens) and mechanically preventing hydrocarbon chain slip of the CTAB as temperature increases. Overall, the increased stiffness of the epoxy because of electrostatically adsorbed clay, which creates physical interlocks on the surface of the

CNCs, shows improved thermo-mechanical behavior above  $T_g$  similar to that of stabilized CNCs in other studies.<sup>35,59,68</sup>

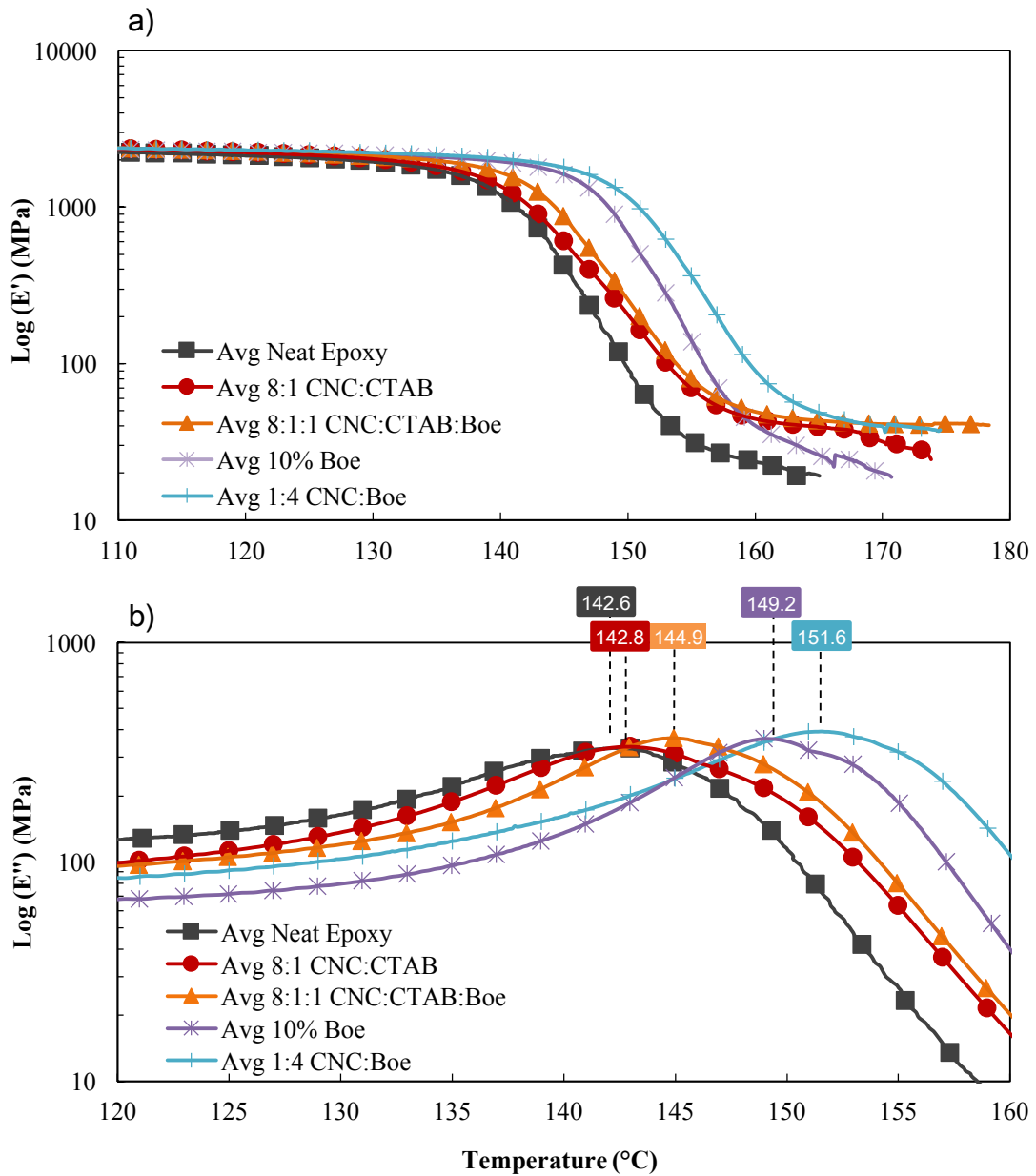


Figure 7: Storage (a) and loss modulus (b) as a function of temperature for epoxy-based composites.

## CHAPTER III

### CELLULOSE NANOCRYSTALS IN POLYPROPYLENE COMPOSITES

In this study, focused on CNCs within thermoplastic matrices, CNC-polypropylene (PP) nanocomposites are prepared and mechanically characterized. Given that good dispersion was desired with PP (the matrix), PP was used to functionalize the surface of the CNCs. Diethylenetriamine (DETA) was used to modify the maleated anhydride side groups of the maleated-anhydride polypropylene (MAPP) by way of a condensation reaction (e.g., nitrogen in the DETA was substituted for the single-bond oxygen in the maleic anhydride). The DETA-modified MAPP (MA) was then added to virgin PP and CNCs in these easily prepared nanocomposites. The benefits to this study include the best known improvements to mechanical properties of solvent-free semicrystalline CNC-PP composites, offering promise for this commodity-resin composite. The reactions in this study occurred in an easily scalable high-shear mixing environment with no organic solvents. The MA-CNC bond benefitted from increased particle-polymer interfacial strength owing to the formation of covalently linked CNC-MA, as evidenced from IR data and improved tensile strength. The CNC dispersion was also improved by way of this treatment method as evidenced from the increase in mechanical properties and confirmed by scanning electron micrographs (SEM). With the combination of mechanical improvements and the ease of fabrication of these DETA-CNC-MA composites, this study offers opportunity for improving nanocomposite performance whereas reducing the environmental footprint of high strength polymeric materials.

## *Experimental*

### **Materials**

Neat polypropylene homopolymer (PP) (Pro-fax 6323; Mn ~180,000, PDI ~0.5) manufactured by Lyondell Basell was used as received. Maleated-anhydride polypropylene (MAPP) (SCONA TPPP 8112 GA; Mn ~75,000, PDI ~0.8) with a 1.4 wt% maleic acid group (MAH) concentration was purchased from BYK Additives and Instruments (Wallingford, CT) and modified as discussed. Diethylenetriamine (DETA) and tetrahydrofuran (THF) were purchased from Sigma Aldrich (Milwaukee, WI) and used as received. Lignin-coated cellulose nanocrystals were purchased from American Process Inc. (Atlanta, GA) and used as received. The size distribution that has been reported elsewhere for woody-biomass derived CNCs prepared by acid hydrolysis is 100–300 nm × 3–5 nm; there are CNCs in the micron-length scales reportedly derived from tunicates, though generic-biomass derived nanocrystals were used for this study.<sup>38,69,70</sup>

### **Polymer functionalization**

The lignin-coated CNCs (CNC-L) were supplied as a very fine powder and were prepared as described in detail elsewhere.<sup>71</sup> Briefly, biomass waste was added to a batch reactor and treated with sulfur dioxide, ethanol, and water to fractionate the cellulose from other materials. Excess lignin, hemicellulose, and proteins were removed by mechanical treatments. The cellulose was unbleached, which retained lignin and increased overall hydrophobicity. The resultant CNC-Ls, were supplied in spray-dried powder and used as-received. DETA is a viscous liquid that was introduced into the

MAPP for this study by way of syringe pump. Figure 8 schematically illustrates the experimental process along with a possible reaction scheme. The CNC-PP composites were fabricated in two steps: (1) varying amounts of DETA were introduced into melted MAPP (Figure 8(a) and (b)) forming DETA-functionalized MAPP (MA) (Figure 8(c)) which was then cooled and pelletized. In step (2): MA (Figure 8(d)) was mixed with varying amounts of freeze-dried, powderized CNCs (Figure 8(e)) and neat PP, and subsequently melt-compounded (Figure 8(f)). The polymer melt was mixed in a high-shear environment (Krauss Maffei-Berstorff ZE 25A twin-screw extruder, Krauss Maffei-Berstorff GmbH, Hanover, Germany), forming MA-functionalized CNC-PP (MA-CNC-PP) composites.

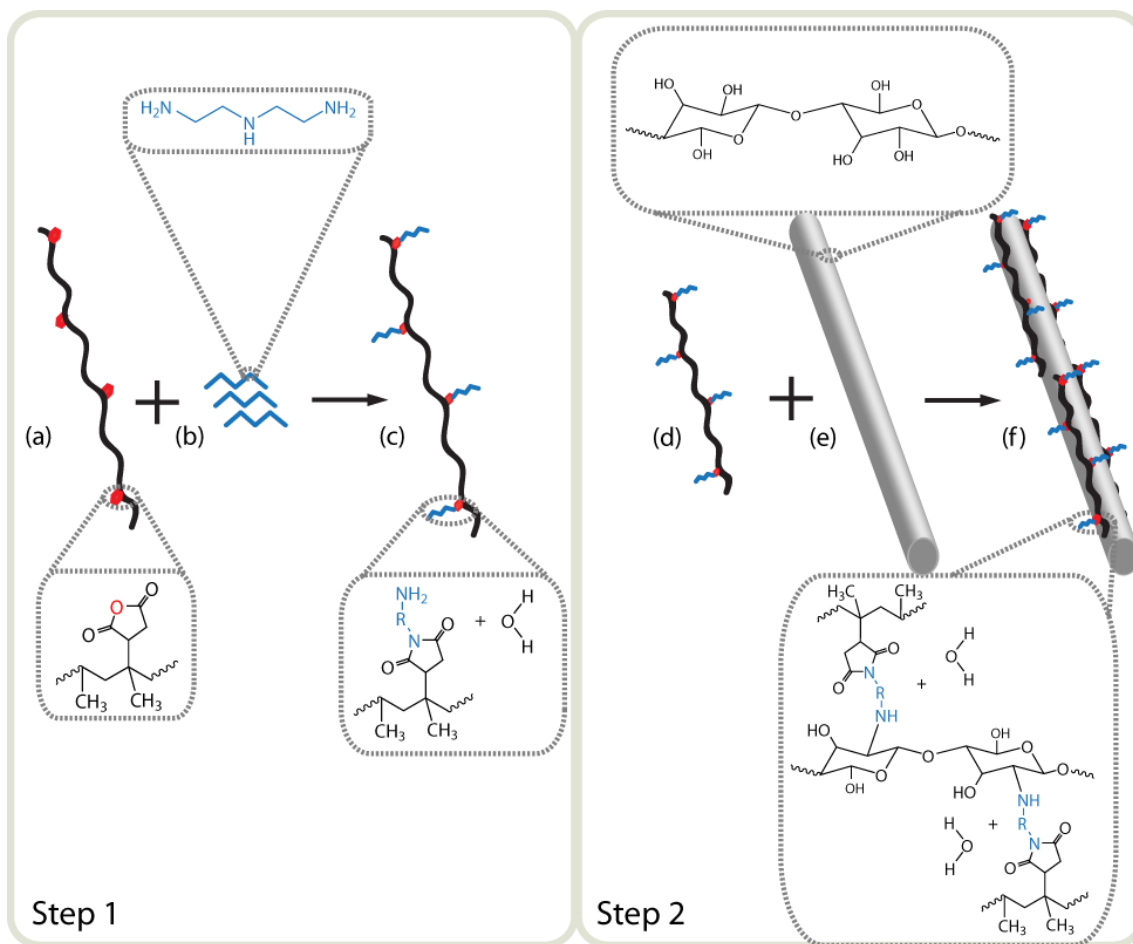


Figure 8: Schematic representation of two-step DETA-MA-CNC functionalization: neat MAPP (a) melt-mixed with DETA (b) creating DETA-functionalized MAPP (and water) (c); DETA:MA (d) added to CNCs (e) which forms a polymer-coated CNC, f).

For Step 1 there were four principle mix ratios of maleic-acid to amine groups (MAH:NH<sub>2</sub>) which were tested to determine both a process-capable mix (e.g., a mixture which would produce a coherent, continuous strand which could be used in subsequent steps) and a trend in which the benefits of the presence of amine groups to the overall composite could be determined. The mix ratios were 2:1 MAH:NH<sub>2</sub>, 1:1 MAH:NH<sub>2</sub>, 1:2 MAH:NH<sub>2</sub>, and 1:3 MAH:NH<sub>2</sub> (MA). The reaction progressed in the barrel of the

melt-compounder at 200°C. For Step 2, there were five principle mix ratios of MA to CNCs which were mixed with neat PP. These mix ratios were selected in order to discern which were more likely to completely cover the CNCs with the MA. The mix ratios were 1:2, 1:5, 1:9, 1:10, and 1:19 CNC:MA. This secondary step was carried out in the same high-shear mixer. Composite pellets were then injection molded in a 55-ton molding machine to produce various geometries suitable for mechanical characterization.

### **NH<sub>2</sub> ⇌ MAH reaction characterization**

Prior to performing reaction-extrusion, various MAH:NH<sub>2</sub> recipes were prepared in a batch-reaction method. In a fume hood, 200 g of each recipe was prepared in THF to prove reaction progression. The mixtures were heated at 85°C and stirred vigorously with a spatula for 14 hours. The THF was then decanted off and the precipitate powder was dried and analyzed by an IR Prestige21 infrared spectrometer from (Shimadzu Corporation, Kyoto, Japan) which performed Fourier-Transform Infrared Spectroscopy (FTIR). Once suitable MAH:NH<sub>2</sub> ratios were selected, these recipes were fabricated without solvents in the melt-compounder. Subsequent to melt-compounding, a composite pellet from each recipe was heated and pressed into a thin-film, approximately 100 µm thick, and analyzed by FTIR to confirm that a similar extent of reaction occurred in the high-shear environment.

### **Composite mechanical characterization**

Tensile tests were performed according to ASTM D638 on an Instron Model 3345 load frame with a 5-kN load cell per ASTM D638 with a crosshead speed of 5.0

mm/min. At least five specimens of each sample recipe were analyzed at each CNC loading (1, 2, and 5 wt%). Specimen dimensions were taken prior to the tensile tests with a Mitutoyo (Aurora, IL) digital micrometer, with 1  $\mu\text{m}$  accuracy. The specimens were tested as injected, pulled from a highly polished hardened-steel mold. Scanning electron microscopy (SEM) was performed using a JEOL JSM-7500F (Peabody, MA) cold emission microscope on representative fracture surfaces from the 5 wt% tensile-test bars.

### *Results and discussion*

#### **Reaction: DETA-MA-CNC composites**

Unlike water-soluble polymer systems that have been studied elsewhere,<sup>14,15,72</sup> PP and CNCs are not intrinsically compatible. However, the reaction between amine groups and maleic acids is well-known and thermodynamically favorable. Primary amines will seek to cleave the single-bond oxygen from the carbonyl carbon, forming an imide group or two amides with secondary and/or primary amines.

Phenomenologically it is clear that the mechanical properties of the resultant composites are greatly improved. Comparative FTIR spectra for the recipes with the most successful mechanical property improvements are shown in Figure 9(a) and (b). There is a substitutionary condensation reaction between the amine groups on the DETA and the cyclic anhydride side groups on the PP (Figure 9(a)). In the case of this study, both primary and secondary amines are present in the DETA. These seek to cleave the oxygen from the cyclic anhydride – particularly the primary amines at the end of the DETA chains – forming amide- and imide-groups on the PP backbone. There is also a



chance of crosslink formation by way of both intra-chain linkages and inter-chain linkages.<sup>73</sup> In Figure 9(a), MAPP is shown, with peaks present at 1850, 1780 and 1720  $\text{cm}^{-1}$ , characteristic of cyclic anhydride groups.<sup>74</sup> The cyclic anhydride groups diminish almost entirely in the presence of the amine: specifically, the peak at 1850  $\text{cm}^{-1}$  disappears entirely. The sharp peak at 1780  $\text{cm}^{-1}$  is attributed to anhydride carbonyl stretching and reduces to a short, broad peak with shoulders at 1770 and 1750  $\text{cm}^{-1}$ . The peak at 1770  $\text{cm}^{-1}$  is attributed to imide carbonyl stretching: the shift from the transmittance at 1780 to 1770  $\text{cm}^{-1}$  (anhydride to imide) is a key indicator for this reaction. The peak at 1720  $\text{cm}^{-1}$  is eliminated entirely. The formation of the strong peak in the 1:1 MAH:NH<sub>2</sub> trace (Figure 9(a)) at 1700  $\text{cm}^{-1}$  is attributed to stretching of the carbonyl groups in the carboxylic acids, and the formation of the peaks at 1580 and 1540  $\text{cm}^{-1}$  are attributed to secondary amides, which help to indicate the possibility of crosslinking, because secondary amides with their available hydrogen atoms are more likely to be present in a crosslinked structure than primary amides.

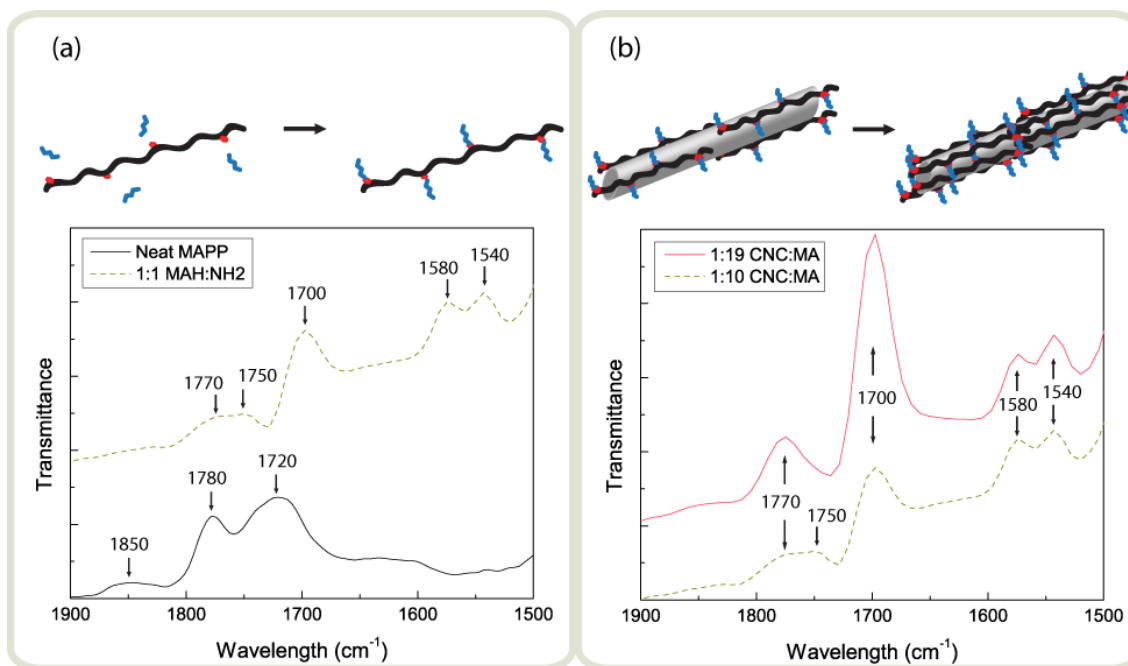


Figure 9: Infrared spectroscopy of the DETA-MAPP-CNC functionalization; the effect of the MAH:NH<sub>2</sub> ratio (a) and the effect of increasing CNC:MA concentration (b). The 1:1 MAH:NH<sub>2</sub> composite in (a) mixed at 1:10 CNC:MA; samples for data in (b) loaded at 5 wt% CNC.

The samples for Figure 9(b) were loaded at 5 wt% CNC, and here the comparative effect of increased particle coverage is shown. The 1:10 CNC:MA trace is the same data from Figure 9(a) and repeated here for ease of comparison. As the coverage of the particle increases from 1:10 CNC:MA to 1:19 CNC:MA, the broad peak at 1770 and 1750  $\text{cm}^{-1}$  sharpens into a strong peak at 1770  $\text{cm}^{-1}$  (the 1:19 CNC:MA sample), indicating increased imide presence in the composite. Additionally, the carbonyl stretching (1700  $\text{cm}^{-1}$ ) is much more prevalent in the 1:19 CNC:MA composite indicating more out-of-plane motion, most likely because of increased steric hindrance from the formation of covalent linkages between the imides, amides, and

former OH groups on the surface of the cellulose particles. Finally, the slight sharpening of the peaks at  $1540\text{ cm}^{-1}$  and  $1580\text{ cm}^{-1}$  (Figure 9(b)) are evidence of greater amide presence, which can be attributed to a higher degree of crosslinking. This recipe had the highest improvements in tensile strength and modulus for composites loaded at 2 wt% (Figure 10(b)). Increases in tensile strength, in particular, are more easily obtained by the presence of covalent linkages; increased crosslinking would also contribute to the explanation of this phenomena.

### **Composite mechanical behavior**

Five samples of each recipe were analyzed via tensile testing according to ASTM D638. Figure 3 shows stress-strain plots for representative specimens containing 5 wt% nanoparticles (Figure 10 (a)) and 2 wt% nanoparticles (Figure 10 (b)). The tensile curves in Figure 10 (a) were taken from samples mixed at 1:10 CNC:MA ratio, and indicate the increase in tensile strength and elastic modulus as increasing amines are introduced to the MAPP. Importantly, overall ductility in the polymer is maintained at  $> 10\%$  strain-to-failure, substantiating the value of the chemical functionalization (e.g., if there were no benefit to the chemistry, the presence of the highly crystalline nanoparticle would increase modulus to the detriment of both ultimate tensile strength and percent elongation). The 1:3 MAH:NH<sub>2</sub> presented the highest tensile strength and modulus at 2 wt% loading (Figure 10(a)) but did not replicate this behavior at higher CNC loadings as did the 1:1 MAH:NH<sub>2</sub> or 1:2 MAH:NH<sub>2</sub> recipes. This could be caused by increased (excess) unbonded DETA, acting as plasticizer, weakening the melt in these recipes. Figure 10(b) illustrates the improvement in mechanical behavior as the CNCs are more

completely coated with functionalized MA, relative to non-functionalized PP. The CNCs for these samples were mixed with CNC:MA functionalized at 1:1 MAH:NH<sub>2</sub> ratio, which offered the highest repeatability at all CNC loadings (though second-highest overall strength and modulus improvements) to the 1:2 MAH:NH<sub>2</sub> recipes shown in Figure 10(a). The 1:1 MAH:NH<sub>2</sub> composites had consistent morphology and bulk composite characteristics ensuring facile handling and production. As the particle coverage increases the ultimate tensile strength and elastic modulus are both increased concurrently and this trend is supported by behavior at the other nanoparticle loadings (e.g., with both 2 wt% and 5 wt% CNCs the mechanical properties of the composite increase both with increasing NH<sub>2</sub> and more complete particle coverage). This behavior is likely caused by the presence of increased covalent linkages, increased cross-linking and greater opportunity for electrostatic interactions at the particle-polymer interface. A related effect derives from increased inter-chain hydrogen bonding as there is a higher quantity of hydrogen-oxygen interactions because of increased imide/amide presence.

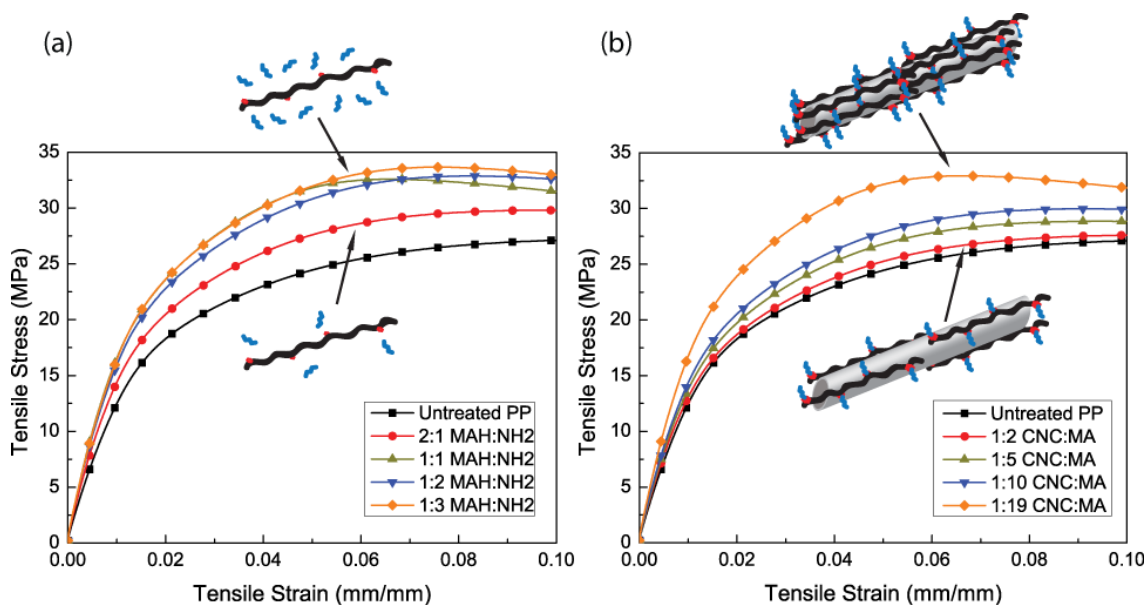


Figure 10: Tensile stress (MPa) vs tensile strain (mm/mm) for DETA-MA-CNC composites showing the effect of MAH:NH<sub>2</sub> ratio (a) and the effect of increasing MA particle coverage (b).

Figure 11 illustrates the modulus and tensile strength values for the composites in this study. Values are shown for neat PP (horizontal reference in each plot) followed by composites loaded with 1, 2, and 5 wt% nanocrystals (Figure 11(a) and (b)). Error bars represent  $\pm 1$  standard deviation. Figure 11(a) and (b) present the average tensile modulus and tensile strength of 1:10 CNC:MA composites, fabricated from 1:1 MAH:NH<sub>2</sub> polymer which offered the greatest repeatability. The elastic modulus increased slightly with increasing amounts of CNCs in the absence of MA (Figure 11(a)). Dramatic increases in stiffness are exhibited when the CNCs are present with MA chemistry (Figure 11(a)) as the elastic modulus increases 74% (from 895 to 1570 MPa). The effect of the chemistry described in this study is evident from these figures, particularly for the tensile strength values, which increase by 32% (from 25.0 to 33.0

MPa) at 5.5% strain for the 1:10 CNC:MA composites (PP+Untreated CNCs in Figure 11(b)). The lack of helpful chemistry is evident from the decrease in tensile strength as additional nanoparticles are added in the absence of the MA chemistry (Figure 11(b)). It is common for stiff particles to increase the stiffness of polymeric composites<sup>75</sup> but without enhancing interfacial adhesion, stiff particles can hurt tensile strength. Modest tensile strength improvements have been reported at low loadings of CNCs (< 5 wt%) as a result of increased crystallinity,<sup>76-78</sup> but higher loadings of CNCs actually show decreased tensile strength.<sup>72</sup> The higher loadings of agglomerated cellulose combined with a weak polymer-particle interface form greater stress concentrations to the detriment of composite performance. Polymer-particle interfacial adhesion is necessary for improving tensile strength and achieved most effectively by way of covalent linkages. Figure 11(c) and (d) describe the effect on the composite when one component of the recipe is removed, as neat PP is plotted along with various composites at differing MA particle coverage ratios (1:2, 1:5, and, 1:10 CNC:MA addition ratios). The tensile strength for composites with 5% CNCs + MA 1:1 MAH:NH<sub>2</sub> is shown in Figure 11(c) and compared against the tensile modulus of PP-MAPP co-polymers (MAPP) and with 1:10 CNC-MAPP-PP composites (e.g., composites fabricated with no DETA). The processing parameters were kept consistent between the runs, for example the MAPP was melt-compounded with neat PP in the first step, cooled and pelletized, and the CNCs were added in a second compounding step to impart consistent heat-histories to the composites. The tensile strength is shown analogously in Figure 11(d).

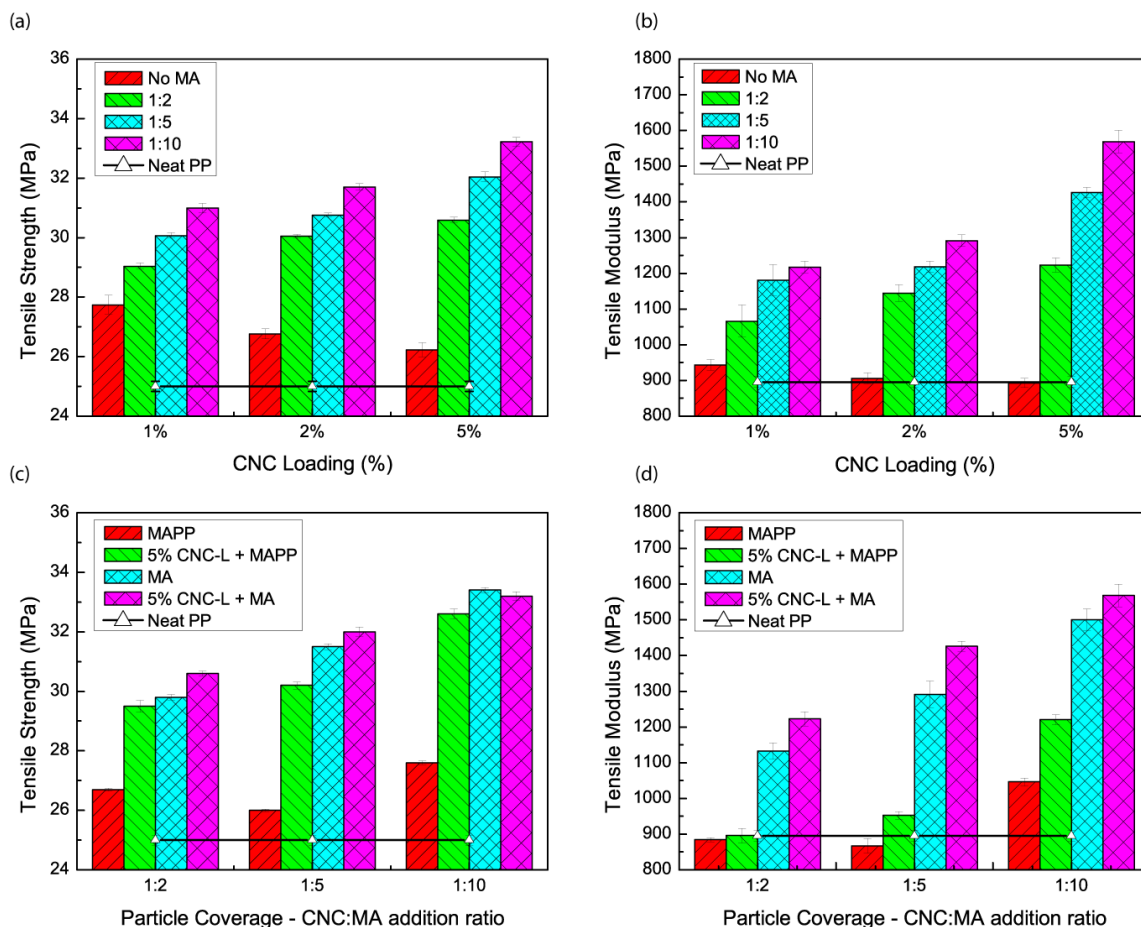


Figure 11: Summary of mechanical properties as a function of CNC loading (wt%) (a) and (b); the effect of individual components of the chemistry (c) and (d). Error bars represent  $\pm$  one standard deviation, based on at least five measured specimens for each composition.

Regarding the PP:MAPP composites, given the differing molecular weights and degree of branching between neat PP and MAPP it was critical to investigate the effect of simply co-extruding the two polymers together. As expected there was a very modest effect on mechanical properties overall, and the increases seen can be explained by the higher molecular weight of the MAPP. Regarding the CNC+MAPP composites, the 1:10 CNC-MA 1:1 MAH:NH<sub>2</sub> composites are shown as those gave the highest

repeatability. The moderate mechanical property improvements which result solely from the addition of the MAPP are most likely caused by the secondary interactions with the OH- groups on the CNCs and the cyclic anhydride groups on the MAPP. These produce particle-polymer interactions of lower bond-strength than the covalent bonds and the cross-links formed from the primary and secondary amides and the imide groups in the DETA-MA-CNC composites.

### **Composite microstructure**

Figure 12 shows scanning electron micrographs of the fracture surfaces of tensile-test specimens. Figure 12(a) shows the microstructure of unfilled PP, Figure 12(b) shows the fracture surface with untreated CNCs in PP. Figure 12(c) and (d) show the evolution of the microstructure as levels of NH<sub>2</sub> are increased. In the composite containing untreated CNCs, PP-rich/CNC-poor regions are evident as regions of agglomerated CNCs are clearly visible (Figure 12(b)). This is consistent with other works that have investigated CNC-PP composites.<sup>78,79</sup> The PP surface appears glassy, whereas the CNC-rich areas have a more granular morphology. Additionally, multiple crystals can be seen in the fracture surface (Figure 12(b) inset). It appears that the failure mode was particle pull-out, with the shape and morphology of the individual crystals matching that reported elsewhere.<sup>14,38,78,79</sup> Figure 12(c) shows the composite with 1:5 CNC:MA and Figure 12(d) shows the composite with 1:10 CNC:MA. The amine functionality has a direct effect on the microstructure of the composite, with individual nanoparticles no longer distinguishable. The morphology of the failures for the composites with increased amine content is more ductile in nature, as evidenced by



out-of-focus regions in the deeper field of view (e.g., there is a greater portion of the micrograph that is out-of-focus indicative of increased ductility in the failure). The composite containing untreated CNCs appears to have failed at the particle-polymer interface whereas the composites which have been treated with DETA appear to have failed at the polymer-polymer interface. Evidence for this is observed in the fibrillar morphology shown in the Figure 12(c) and (d) insets.

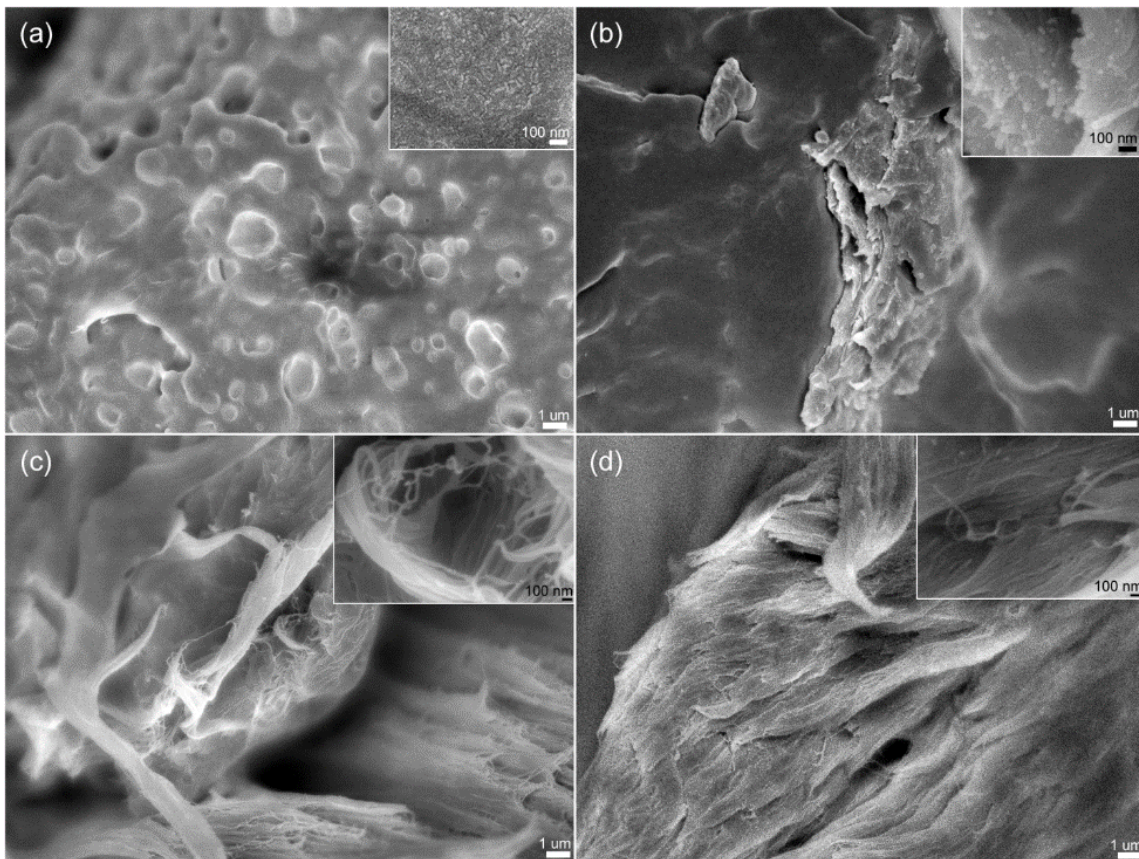


Figure 12: Composite microstructure as a function of CNC and DETA-MA-CNC treatment. Neat PP (a); PP with untreated CNCs (b); PP microstructure with 1:5 CNC:MA (c); PP microstructure with 1:10 CNC:MA (d).

## CHAPTER IV

### CELLULOSE NANOMATERIALS IN THE MARKETPLACE

Given the efforts and results of the work reported thus far, it follows that pre-commercial technology such as nanocellulose-polymer composites require scientific investigation and the investment of time and effort to be brought from an idea to commercial application. This investment comes in stages and as time progresses, the initial waves of financial support, normally awarded from federal funding agencies, begin to fade away as solutions are found to early stage problems. Figure 13 illustrates the typical investment pathway of a new invention.<sup>80</sup> As the efficacy of a given idea is unknown at the start of exploration of same, the dedication of resources to the pursuit is always high-risk, so much so, that industrial and private parties typically shy away from these types of pursuits. Academic and other public research institutions are perfectly equipped to perform the early stage (fundamental) research needed to answer the early questions posed. If the solutions found prove technically effective, the idea moves into an applied research phase, and this work may still be too early stage to be funded by existing commercial ventures. Therefore, there is often a new venture that forms to take the invention through the remaining development phases and into commercial launch. Normally, a new venture is formed at the tail end of the first wave, and the activities typically performed in the so-called “Valley of Death” (i.e., the gap between the first and second waves) include prototypes, validation builds, alpha- and beta-testing and initial scale-up work as required to fabricate repeatable instances of the solution produced in the laboratory.

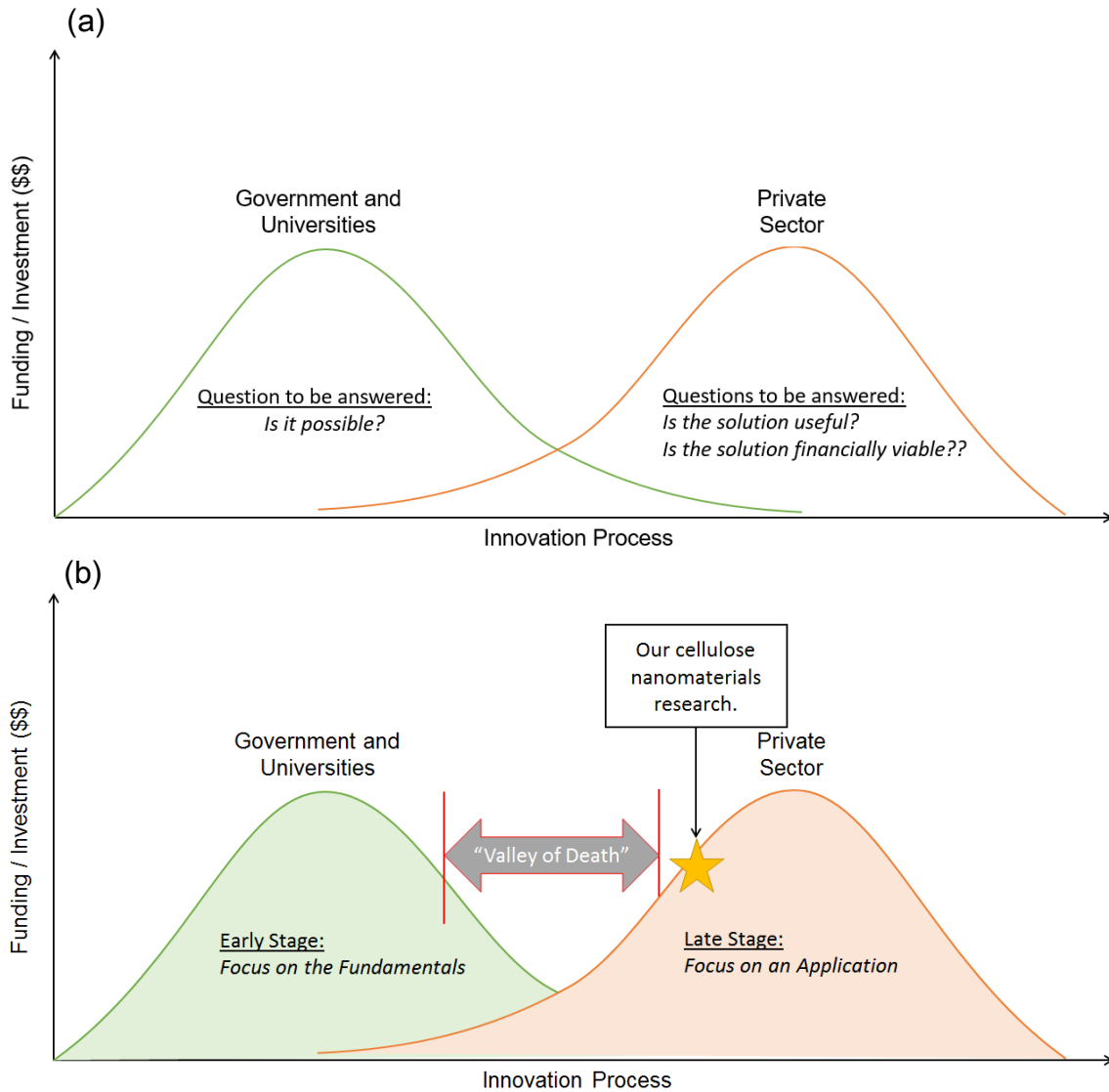


Figure 13: Investment money as a function of an invention's position in the overall innovation process (a). Major funding sources, research stage and overall position of the CN-polymer composites in this work (b).

One of the principle tenets of the approaches taken with the current work is a keen focus on the commercial marketplace for hierarchically higher-ordered devices incorporating CNs and, in particular, bulk composites. Bulk composites are significantly different from thin-film composites in that the thickness of the fabricated device is

usually of the same length scale as the other physical dimensions of the device. There is not yet any commercial bulk composite within which CNs have successfully been incorporated. Therefore, it is of critical import to the cellulose community from an adoption standpoint that a market presence establish in order to fund additional areas of research and development, pulling new inventions to the fore.

*Potential uses for composites with CNs*

An example end-use case for the high-volume manufacturing (HVM)-focused approaches applied in this work is in the application of CNs in polymer composites for the automotive industry. The automotive industry is motivated to adopt new, lighter weight materials for use in all vehicles because of stringent CAFE fuel economy standards for future vehicles. Typical vehicle curb weights have grown over the past several decades as increasing safety equipment, larger engines and chassis dimensions have all become more mainstream. Vehicle weight reduction has been identified as a key enabling factor to reaching future stringent fuel economy requirements. The materials most commonly considered as candidates for light-weighting in automobiles are carbon fiber composites, short- and long-glass fiber composites, aluminum and aluminum/magnesium alloys. All of these materials have found uses (or potential uses) in the vehicle, but they are typically significantly more expensive than the parts they are intended to replace. Additionally, especially in the case of carbon fiber composites, the processes used to manufacture these parts are low-volume, time/resource-intensive processes that are difficult to scale economically. The approaches highlighted in the CN composites developed in this work are attractive to the current market because these

composites utilize existing high-volume manufacturing processes such as melt-compounding and injection molding, whereas providing components with improved mechanical performance and lower density. For instance, automotive components are often fabricated from polypropylene matrix loaded with 20% short glass fibers. Two additional advantages to automotive components manufactured with the HVM approach utilized in this work are (1) significantly longer tooling life due to lower abrasion and (2) lower equipment operating costs because of lower viscosity of the injected polymer composite, both as compared to legacy, glass-filled polypropylene composites.

#### *Scale up plans*

Bulk composite samples for this work were fabricated on a 25-mm twin-screw co-rotating extruder, with a 46:1 length:diameter (L:D) ratio. Thermoplastic extruders with analogous L:D ratios are common throughout the automotive industry, with barrel diameters of up to 96 mm. The material throughput rates on these machines exceed 700 lb/hr, meaning the annual production rates are on the million lb scale. The production methods utilized throughout this work are so-called ‘drop-in’ preparation methods, meaning the material feed techniques apply to larger machines and the material mix ratios scale linearly with machine throughput.

#### *Cost analysis: Raw material supply and pricing*

The volume and cost projections for raw materials is given in Table 2. Mature costing for raw materials is expected to be approximately \$1.37/lb. Projected costing for raw materials is approximately \$1.09/lb based on improved formulation optimization. As shown in Table 2, the largest cost component for the composite is the MAPP. This

provides the cost motivation to improve the efficiency of the interaction of the MAPP-Amine with the nanocellulose.

Table 2 - Raw Materials Cost Summary at Current and Projected Phase II Formulations

Raw Materials			Current	Projected
Item	Cost		Wt%**	Wt%**
PP Resin Matrix	\$ 0.90	/lb	70%	85%
Nanocellulose*	\$ 1.00	/lb	5%	5%
M.A.	\$ 2.74	/lb	25%	10%
Amine	\$ 0.24	/lb		-
MAPP	\$ 2.50	/lb		-
<b>Total</b>			<b>\$1.37 / lb</b>	<b>\$1.09 / lb</b>

\* Mature Pricing from Commercial Plant (Q1 2018)

\*\* Potential Composite Formulation

### *Competing technologies*

There are multiple companies supplying myriad components to the automotive industry, and each seeks to address the need for more fuel-efficient vehicles. Direct competition includes manufacturers offering lightweight performance materials such as other-reinforced plastic composites: cellulose and other natural fibers, chopped glass fiber, and chopped carbon fiber. Indirect competition includes those making parts from aluminum and high-strength steel (HSS). These materials cost more and have a higher density than CNCs, and though mechanical properties are strong, the former two allow space for innovation of new CN-focused materials such as the composites highlighted in this current work.

Table 3 reflects the cost and competitive advantage of cellulose nanocomposites (top row) in comparison to other materials listed.

Table 3 - Competitive Summary Table - Automotive Structural Materials

	Provider	Product Name	Price	Mech. Properties	Final Part Weight	Processability	Sustainability / Environmental Impact	Availability
Current Competition	Cellulose & Natural Composites							
	Essentium Materials	Axium Nano*	\$1.25 - 3.50 **	/lb***	●	●	●	●
	Weyerhaeuser	THRIVE composites	unavailable		●	●	●	●
	Chopped Glass Fiber Composites							
	LyondellBassell	Hostacom	\$1.05 - 3.50	/lb	●	●	●	●
	Owens Corning	NORYL PPX			●	●	●	●
Dupont	Zytel HTN	●			●	●	●	
Future Potential Competition	Chopped Carbon Fiber Composites							
	Celanese	Celanese	\$5 - 10	/lb	●	●	●	●
	Toray (Zoltek)	Panex			●	●	●	●
	Teijin Limited	Tenax			●	●	●	●
	Metal (Steel, Aluminum)							
	General Motors		\$2 - 12	/lb	●	●	●	●
Flex-N-Gate		●			●	●	●	
Toyota		●			●	●	●	

\* Trade name still pending

\*\* Pricing given in ranges for several reasons, primarily due to different resin matrix systems

\*\*\* Average mature pricing estimates, see Financials Section (4.4) for more information

*“Valley of Death” commercialization plan*

To move this work from early stage laboratories to the commercial marketplace, partnership with an existing startup venture was employed. Essentium Materials (EM) specializes in developing material technologies that are stronger, cost less, and are faster to produce than chopped glass fiber composites. Sourced from 100% pure nano-scale, crystalline cellulose, EM has a solid, patent-pending process to make sustainable nanocellulose-reinforced composites that significantly reduce the weight of structural automotive components. The initial commercial product under development from this work is an injection grade, nanocellulose-reinforced polymer-composite pellet for the automotive industry, followed by other customers served by the global glass and chopped carbon fiber composites industry.

## *Customer analysis*

### **Customer need**

The single greatest factor influencing new technology development for automakers is regulatory pressure to improve fuel efficiency of their vehicles. By 2025, automakers are expected to increase the fuel efficiency of their cars and light trucks to an average 54.5 mi/gallon.<sup>81</sup> The push to ‘lightweight’ vehicles is therefore stronger than ever, with automakers looking to shave hundreds of pounds off of every car. An obvious strategy to help achieve this is via weight reduction, because it has been shown that every 10% reduction in vehicle weight can cut fuel consumption by about 7%, resulting in CO<sub>2</sub> savings of 25.3 kg for every kilogram of weight reduced over the vehicle lifetime. Whereas design plays an important role in this strategy, materials selection is arguably more significant. Additionally, there are other potential threats to incumbent structural materials. The world price of steel is expected to continue to increase with the increasing price of crude oil, squeezing commercial margins for metal-stamped parts.<sup>82</sup>

*Nanocellulose composites developed in this work are 10% lighter than mechanically similar glass-fiber composites. These products contain only 5% nanocellulose, compared to 20% loaded glass fiber composites.*

### **Current solutions**

Although there are competitive materials designed to meet some of the light-weighting demands (carbon-fiber composites, glass-fiber composites, and metals like aluminum), the materials and/or their manufacturing processes often come at a much



higher price, with considerable environmental drawbacks. Table 4 shows incumbent and current solutions for structural interior parts and their shortcomings.

Table 4 - Current Technologies Being Used and Their Shortcomings

Current Material/Technology	Cons
Aluminum / other Metals	Heavy, high manufacturing costs
Short glass fiber composites	Heavy, abrasive on manufacturing equipment and tooling
Long glass fiber composites	Heavy, abrasive on mfg equip and tooling, difficult to manufacture because of high viscosity
Chopped carbon fiber composites	High materials cost, abrasive on mfg equip and tooling, difficult to manufacture, energy intensive processes

Today’s high-performance and lightweight materials come at a higher price than the projected mature costs of CNs. Carbon fiber composites are both expensive to procure and have long cycle times during fabrication. One automaker which is making significant investment in the renewable materials space is Ford Motor Company (Ford). Ford exhibited interest and, as mentioned in the Acknowledgements, contributed significant research funding to this work. EM is a registered supplier to Ford providing technology innovation and development. Specifically, EM has conducted more than two years of sponsored research in conjunction with a joint development agreement (JDA) with Ford.

Further discussion detailing the efforts leveled to date between EM and Ford, as an example of the commercialization process for CN-polymer composites, are provided.

From the time of this writing, Ford is hoping to launch initial parts in the next 12–18 months for a thin-walled structural instrument panel bracket part. General Motors (GM) is also investing research dollars into this technology with university institutions. GM may become a second early adopter of this technology should commercial scale-up prove successful.



Figure 14: Instrument panel – target automotive part.

The initial target application is structural automotive thin-walled parts such as instrument panels (IPs) that have a high strength and stiffness (Figure 14).

*Industry overview & customers*

**Industry structure & value chain**

The initial product offering of CN-polymer composites fits most nearly within the plastics for structural automotive interior parts fits within the Motor Vehicle and Interior Trim Manufacturing (NAICS code 336360) submarket. To facilitate production of the proprietary blends discovered through this work, EM has secured an agreement to cost-effectively lease compounding equipment line time from GDC, a current Tier 1 supplier to Ford and other automakers. Once the technology is validated through temporary usage of the production line, a potential revenue pathway out of the “Valley of Death” would be to license the technology to GDC and/or other Tier 1 suppliers. A summary of the value chain for automotive interior and trim parts is given in Figure 15.

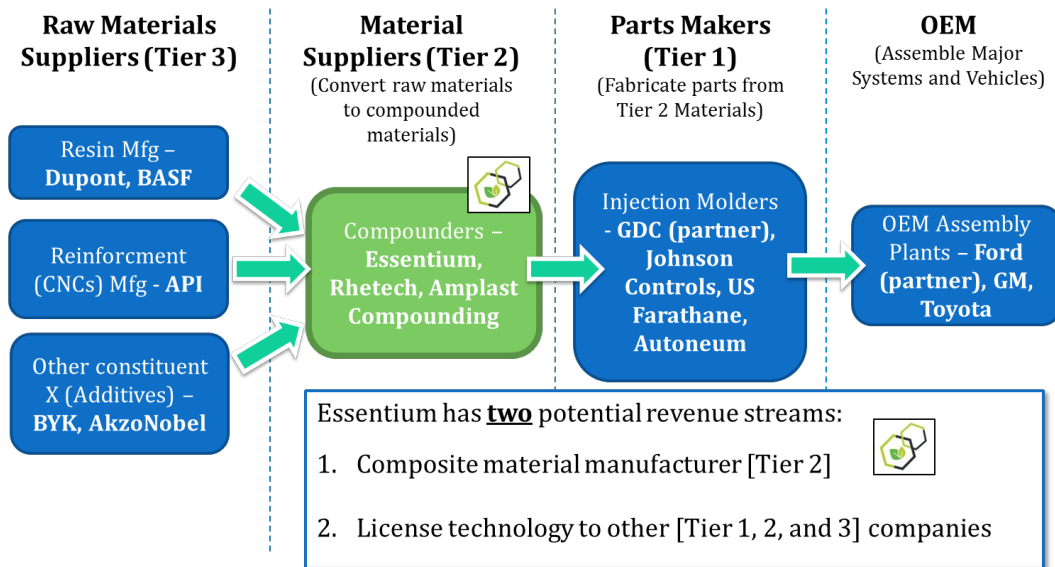


Figure 15: Value chain for structural automotive interior parts.

Figure 15 illustrates a potential commercial value stream for the CN-polymer composites developed in this work, showing delineations for supply Tiers 1–3 and original equipment manufacturers (OEMs). In addition to EM, there are other companies in North America that are actively scaling production of NCs. For instance, American Process, Inc. (API) has demonstrated cost-effective NC supply, some of which was used for this work.

### **Sales channels**

GDC currently sells products primarily through an automotive sales rep company, RWP Kinsale. RWP Kinsale has strong relationships throughout the automotive ecosystem. There are other potential options through Ford’s network of partners (especially for the revenue-from-licensing option), but this would offer the least barriers to entry and most straightforward starting point for getting parts to our immediate targeted customers.

### *Market analysis*

#### **Market definition**

The global nanocomposites market is a very rapidly growing technology industry. Although nanocomposites have been used commercially since Toyota first introduced nanoclay into polymer composites in the 1980s, recent advances in the ability to characterize and manufacture nanocomposites have opened the door to many new applications. Nanocomposites are now finding uses in a wide range of automotive applications, because of their ability to significantly enhance many different properties such as: tensile strength, modulus, heat distortion temperature, color/transparency,

conductivity, flame retardancy, barrier properties, magnetic properties, and anticorrosive properties.

The automotive market segment is a good candidate for commercialization of this work for several key reasons:

1. The industry must light-weight its vehicles, and high-performance nanomaterials, which are easy to manufacture, have enormous potential to meet this need.
2. EM has previous successes with composite materials in the automotive industry with multiple industry partners to help lower the barriers to entry for new materials.
3. Current “state-of-the-art” light-weighting materials (glass-reinforced composites, carbon-fiber composites) have long production cycle time, high cost, and are difficult to manufacture. EM’s nanocomposites are cost competitive and easy to manufacture.

### **Market size**

At the time of this writing, the nanocomposites market applications are highest for automotive parts, packaging, and electronics, with market shares of 51.4%, 22.5%, and 13.8%, respectively. The estimated total domestic nanocomposites market was \$1.2 B in 2013. The automotive parts sub-market was \$617 M in 2013.<sup>83</sup>

The served available market (SAM) size was calculated using a bottom-up approach looking at recent trends within the automotive industry in the United States and the market growth of nanocomposites as a whole. The number of light vehicles in the United States is expected to grow steadily over the next decade, with sales estimates

reaching 17.4 million by 2017, up from 16.4 million in 2014. Global sales are similarly forecasted upward, with China leading the way with large growth potential.<sup>84</sup> There have been an average of 330–380 pounds of plastics and plastics composites in North American light vehicles each year since 2003, and that number is expected to continue to grow, especially as higher performance materials become more available and more affordable and can replace heavier metal parts. Calculations for this work used an average of 350 pounds of plastics per vehicle, where initially 15% (~53 lb) of those were suitable for this CN-polymer technology (it is estimated that around 110–120 pounds per vehicle are PP, PA, and their composites, so it is estimated less than 1/2 of PP and PA applications would be applicable). By 2020, it is estimated that as much as 30% of the plastic in the vehicle could be potential nanocomposite applications. These numbers agree with the global nanomaterials market study that estimates the automotive nanocomposite market was ~\$617 M in 2013 and could be as high as \$1.7 B by 2019.<sup>85,84</sup> Initial product offerings are domestic, but OEMs (including Ford) have made global standardization of materials a priority, and would eventually seek to propagate this material globally.

Research shows that the global nanocomposites market is expected to grow to \$4.2 B (USD) by 2019, with a five-year combined annual growth rate (CAGR) of 24%. The global volume for nanocomposites is expected to reach 1.5 billion pounds by 2017, and growth is expected to be driven primarily by rising levels of government participation in R&D funding, the increased role of private VCs, technology advancements netting reductions in production prices, and increased demand for high

strength structural materials across a broad range of end-use markets.<sup>86</sup> The distribution of the market is shown in Figure 16.

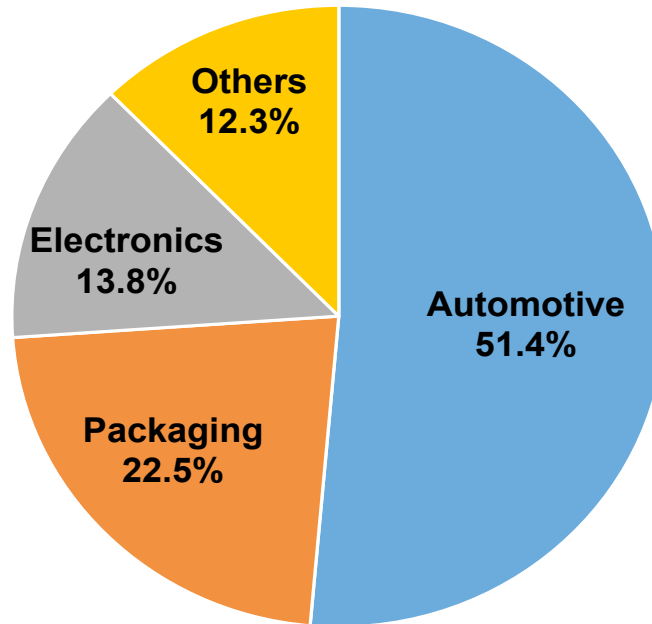


Figure 16: US Market segmentation for nanocomposites (2013).<sup>84</sup>

### **Market growth & trends**

The automotive market is expected to strengthen with strong car sales and more efficient vehicle production in the coming years. Material consumption for vehicles has moved towards lighter materials with better strength-to-weight ratios (STWR).

Regarding vehicle material consumption, there are several key trends to note:

- The steady decline of “regular steel” usage, because of its poor STWR compared to aluminum and high- to medium-strength steels (and even plastic composites): from 44.1% in 1995 to 35.8% in 2011.

- There has been a significant increase in the use of aluminum and high- and medium- strength steel replacing regular steel and iron castings. Improved composites could displace this growth in some applications.
- Plastics and plastic composites' industries are showing healthy growth as new applications become possible with higher performing composite materials (including nanocomposites). In 1995, an average 240 pounds of plastic and plastic composites were being used in the vehicle. That number has increased to 377 pounds per vehicle in 2011, with continued growth likely in coming years.
- The use of reinforced plastic composites is steadily on the rise, with polypropylene (PP) and polyamide (PA) resins being the highest consumed, approximately 545 million pounds in 2014, and projected 614 million pounds by 2019.<sup>84</sup>

### **Barriers to market entry**

There are companies in the materials industry investing in the development of the technology for nanocomposites, both within automotive and other industries. There are several large companies that make up over 50% of the market share for carbon fiber based composites (e.g., Lear and Visteon). By partnering with existing players in the industry (e.g., Ford and GDC) the commercial opportunity for this work can be maintained with low overhead, high efficiency, and high agility whereas utilizing existing infrastructure for sales and manufacturing channels from these established companies.



### *Intellectual property landscape*

In 2009, there were eight patents published regarding CNCs, and in 2010 there was a 100% increase, followed by a 70% increase in 2011. The main application for CNCs is composite materials (it should be noted that these applications range from pharmaceutical to absorbents to structural uses).<sup>87</sup>

There are two particular patents of interest related to the technology included below, namely of incorporating CNCs into plastic composites or in the preparation thereof:

- *International Patent No WO2013/037041: “NCC-Based Supramolecular Materials for Thermoplastic and Thermoset Polymer Composites” – a method for the preparation and use in thermoplastic & thermoset composite systems of “supramolecular materials” of CNCs and one or two polymers synthesized by in situ surface graft copolymerization exhibiting low polarity and high hydrophobicity.* This patent is pursuing similar end-goals of improving composite performance but using a different approach. This technology path grows polymer chains directly onto the surface of the nanoparticle that can then be incorporated into the polymer matrix. The technology path of this work is different in that a melt-mixing approach is used to promote dispersion and achieve improved composite performance. An advantage of this work is the lower barrier to wide-scale economical production of the composites.<sup>88</sup>
- *US Patent No 8372320B2: “Method for Drying Cellulose Nanofibrils” – a method for producing dried cellulose nanofibrils through a spray-drying process.* This patent

is for the preparation of nanofibril cellulose (as opposed to CNCs, nanofibrils have larger dimensions and do not undergo the acid hydrolysis process to achieve pure crystals) via a spray-drying process for ease of use in a conventional manufacturing extrusion process.<sup>89</sup>

### **IP due diligence and freedom to operate**

This work has been considered in light of all of the significant players in the relatively small nanocellulose industry (e.g., CelluForce, University of Maine, Weyerhaeuser, etc.), as well as keywords related to nanocellulose and composites. Additionally, a historical nanocellulose patent review published in 2013 indicates approximately 30 patents published in 2011 and fewer in previous years, which seems consistent with the quantity of patents related to cellulose nanoparticles and its applications.<sup>90</sup> Because of this competition, market execution with these initial automotive launches and ability to form partnerships (and maintain partnerships in the case of Ford) with the key players will be necessary, sustainable competitive advantages that will help this new technology cross the “Valley of Death” successfully.

### **Intellectual property developed in this work**

Although much work in academia regarding nanocellulose particles in polymer composites has been conducted, there is no known significant intellectual property generated with regard to our approach to commercial scalability. In June 2014, EM filed a provisional patent application with the USPTO entitled “Cellulose Nanocrystal Polymer Composite” (App # 62007224). This provisional patent was filed as a non-provisional patent earlier in 2015. Additionally, two provisional patent applications were

filed in 2015, including a patent covering the nanocellulose and MAPP-Amine technology from Chapter III.

*Finance & revenue model*

**Estimate of funding needed**

EM is positioned to initiate scale-up activities for CN composites in this work. Given below in Table 5 are a list of technical, intellectual property, marketing/business, and manufacturing milestones to be achieved within the next three years, along with the estimated required funding and anticipated funding sources for each.

Table 5 - Milestones Summary Table

	Milestone	Timeframe	Financing Approach	Amount of Funding Required
Technical	Composite Optimization	2016	Grant & research contract(s)	\$1 M
	Optimize composite loading ratios	2016	Grant & research contract(s)	
	Experiment with additive packages	2016	Grant & research contract(s)	
	Automotive OEM (Ford) Material Specification approval	2016	Grant & research contract(s)	
Intellectual Property	File newest patent application	2015	Internally funded	\$5 k
	File additional patents as needed	2016+	Internally funded	\$15 k
Marketing / Business	Ford JDA funding renewal	2016	Ford JDA contract	\$50 k
	Initial OEM platform launch	2017		
	Launch with 2nd OEM Customer	2018	Internally funded	\$20 k
Manufacturing	Raw materials sourcing & supply agreements with API	2016-2018	Capital Raise / Phase II	\$2-3 M
	Add secondary extruder to process M.A.	2017	Capital Raise / Phase II and Phase IIB	
	Initial low-volume production	2017-2018	Capital Raise	\$1 M
	Ramp up manufacturing	2019-2020	Joint Venture with Partners / Capital Raise II	\$20 M

EM has already completed a significant portion of aligning the value chain and understanding the necessary steps remaining to cross the “Valley of Death.” The largest remaining risk is the technical process development piece.

Because of the nature of the relationship with GDC, EM has access to lease the compounding line capable of producing up to 3 million pounds annually of composite CNC pellets. The lease of this commercial line positions EM as the Tier 2 materials supplier. This arrangement keeps capital costs low as GDC is an experienced and established player. Through this agreement, EM-paid employees will be overseeing the production of the material as well. This way EM can maximize the infrastructure in place to handle the first parts and platforms. As production increases EM can purchase a similar line as revenue and sales warrant. EM has access to VC and Angel investment communities which can facilitate a fund raise on the order of \$3 MM. This event could also be under the form of a joint venture with multiple partners, but would become more formally defined over the course of the Phase II/IIB project.

#### **Evidence of support for the current work**

**Ford Motor Company** has funded research and development work being completed by EM as well as assisted with supply and value chain development to launch products within the automotive sector. Ford continues to be an interested partner and will conduct part testing and verification from prototypes produced for the initial instrument panel part being targeted. For this trial Ford will provide a prototype tool as well as the finished tooling for full-scale manufacture.

**GDC** is a manufacturing partner that will be heavily involved in the early production and scale-up of this technology. GDC's leadership in innovative manufacturing methods for automotive parts has fueled their rapid growth over the last 15 years. GDC has multiple sales avenues to many of the major automotive OEM's in the US and Europe. Additionally, EM has shared intellectual property and trade secrets for multiple technologies with GDC. GDC will provide production-scale compounding for the initial vehicle platforms and potentially the part molding as well.

**RWP Kinsale** is helping EM with product-market fit and strategic sales advice. RWP will represent EM with sales in the automotive space. RWP has demonstrated over the past 20 years a capability to sell renewable composite materials for interior, exterior, and underhood automotive applications. RWP was instrumental for increasing GDC revenues from \$5 million to \$70 million in the period from 1995 to 2013.

**American Process Inc.** is EM's nanocellulose supply partner. API has the capability of producing a higher quality nanomaterial compared to any of their competition in North America at their demonstration plant. API is in the process of constructing a commercial plant to make the nanocellulose cost equivalent to traditional resins.

#### **Method of revenue generation**

The primary method of revenue generation from this technology will be direct sales of the composite material to Tier 1 automotive suppliers and other injection molding companies. However, because of the technology maturity and the relatively slow adoption process for new materials into the automotive industry, it is not likely that product revenues will be generated until 2017–2018, and these would initially be a low-

volume automotive platform or partial platform, estimated at approximately 10,000 units/year. Prior to that, sales in 2016 would be prototype material for trials. Once the initial platform launch is successful, more automotive platforms would work the material into their build cycles, assuming the business case can be met.

*Model for projecting revenues for 3 years post Phase II*

**Revenue**

*Market share projections*

These projections are consistent and reasonable based on conversations with a candidate first customer for the technology developed in this work. For example, Ford is positioned to be the initial automotive customer. Other OEMs may also become customers after Ford's initial platform launches, through existing sales channels at RWP Kinsale and others.

*Product pricing strategy*

The incumbent product which is being targeted for replacement is chopped glass-filled automotive composites. The primary motivation is to replace competing products that are composed of 30% glass-polymer composites. Glass fiber composites are a mature product and fairly inexpensive. Mature volumes of new CN-polymer products can expect to approach the price of glass fiber composites as the price for nanocellulose is expected to drop exponentially with the completion of API's commercial nanocellulose plant in Q1 2018. Mature pricing for lignin-coated CNs is projected to approach ~\$1 per lb, with an annual capacity of 10,000–30,000 tons.<sup>88</sup> Prior to that, pricing for prototype quantities will be higher. This is normal for a candidate automotive

parts pricing progression.

## CHAPTER V

### CONCLUSIONS

#### *On the general approach*

Much scientific research effort in the academy is performed in the pursuit of fundamental, early-stage knowledge creation. Answering the question of: *Is it possible?* Academic research labs are particularly well suited for this purpose, in fact. As is often bemoaned on the streets outside of many of the world's finest educational institutions; however, at times a loss of context can occur when the pursuit of new scientific knowledge ceases upon addressing possibility alone. This need not be the case, as a secondary benefit accompanies the pursuit of early stage scientific research in academia, and that is the benefit of co-location of multiple branches of the academy, i.e., engineering, the sciences, and business. Some researchers find they are able to glean the most value for the academic and commercial communities by concurrently developing not just new ideas and knowledge, but new structures, new solutions providing both scientific and economic profit. In the case of the work performed and written upon herein, that has been the intent. New scientific discoveries have been made and are documented. To add context to this work, much congruency exists between these discoveries and the formation of new business ventures over the same period.

In sum, the scientific work accomplished over the period is joined by commercial work of similar scope:



- Two new companies co-founded by Mr. Blake Teipel and others during the period: Essentium Materials, June 2013, and TriFusion Devices, in January, 2016.
  - Essentium Materials:
    - Has been awarded \$900k from the National Science Foundation for commercial scale-up effort to take the scientific research discussed in this work across the “Valley of Death” to commercialization.
    - Has grown from four team members to fifteen team members during this period.
  - TriFusion Devices:
    - Applies analogous commercialization principles discussed in Chapter IV to different scientific work needing to cross the “Valley of Death.”
    - This other work combines novel uses for polymer-nanomaterial composites with additive manufacturing of biomedical devices
      - To exemplify progression of this new knowledge into the commercial arena, TriFusion Devices was awarded first-place finish at the:
        - 2015 Raymond Ideas Challenge

- 2015 Southeastern Conference  
Entrepreneurial Pitch Competition
- 2016 Baylor New Venture Competition
- 2016 Rice University Business Plan  
Competition
- TriFusion Devices was also awarded first runner-up:
  - 2016 Texas A&M New Venture  
Competition

These commercial pursuits bear mention herein because the best and highest progression to the academic community occurs when scientific research progresses from the laboratories into the commercial marketplace. Well-trained scientists who gain expertise in commercialization enliven the overall research community and aid in drawing out the full potential for thriving and flourishing of all people, including those throughout the academy.

The scientific work presented in Chapter II and Chapter III is summarized in the subsequent sections.

#### *CNC-boehmite*

Many nanoparticles are able to stiffen epoxy matrices and gains have been reported with both renewable and synthetically derived particles. In the present study CNCs stabilized with nanoclay are shown to improve stiffness, strength and thermal stability whereas maintaining elongation of a model epoxy system: the synergy of the

CNC:nanoclay system is primarily caused by increased mechanical interface between the polymer and the filler. This renewable system is marked with high potential for straightforward, cost-effective manufacturing lowering the use of surfactants whereas increasing the market penetration of polymeric nanocomposites. Applications such as automotive components, building construction products and durable consumer goods are poised to benefit from these new systems.

#### *CNC-PP*

In the present study, DETA has been used to alter the functionality of cyclic maleated-anhydride side groups attached to polypropylene. Cellulose nanocrystals were then added and melt-compounded in a later step. This chemistry improved the stiffness and tensile strength of the resultant composite, whereas maintaining a high strain-at-break value ( $> 5.5\%$ ). The formation of covalent linkages at the particle surface, in conjunction with crosslinking and secondary bond interactions, synergistically strengthens and stiffens PP composites. Additive manufacturing, automotive applications, construction materials and consumer products are likely to benefit from the improved properties afforded by using this solvent-free system to disperse/strengthen cellulose nanocrystals in polypropylene. In additive manufacturing, specifically, CNCs can be used at 5 wt% without any adverse effects on processability whereas exhibiting increased properties.<sup>91</sup> Moreover, the chemistry is promising for other high volume thermoplastic polymers such as polyethylene, opening up even more possibilities for utilizing this abundant and sustainable reinforcement material.<sup>92</sup>

The commercial scale up efforts presented in Chapter IV are summarized as follows.

*Commercial scale up efforts to date*

In Phase I of an SBIR program, EM developed a nanocellulose-reinforced composite that meets the tensile strength requirements for a 20% short glass filled polypropylene at a weight savings up to 13%. Achieving a 30% short glass fiber replacement would have a 20% weight savings. Phase II technical objectives will be focused on (1) meeting all Ford Engineering Material Specification performance requirements for 20% and 30% glass fiber composites, (2) raw material (maleic anhydride polypropylene (MAPP)-Amine) supply optimization, and (3) manufacturing development for commercial scale up. At the conclusion of the Phase II, EM will have gained automotive approval with our initial customer, and be seeking to launch a first part on a vehicle.

*Broader impact*

Nanocellulose-based composites are replete with social, educational, and scientific benefits. The target application is to replace heavy glass reinforcement in polymeric composites with CNCs for car parts, providing lighter weight vehicles with increased fuel efficiency. This nets strong environmental benefits. On-going research on the production of CNCs from various wood sources have resulted in significant reductions in cost (with more coming), making CNCs an increasingly attractive functional natural filler, the processing of which, will provide jobs in both manufacturing and the high-tech sector. Successful implementation of CNCs into composites could not only lighten vehicles and reduce environmental impact, but also

transform a waste stream into high-value materials helping meet current societal needs whereas sustainably creating new, less harmful materials for future generations.

*Summary from Appendix: Thermal interface materials*

The commercial market for TIMs is large and growing, expected to double in size to at least \$3.7 Bn by 2025. The performance of this technology against the key metric for this industry, thermal conductivity, in conjunction with the second key metric, surface conformance (softness), vastly exceed the nearest known solution. Key development risks remain and will need to be mitigated through robust, objective innovation.

*On the author's professional philosophy*

Evidence based entrepreneurship is the most highly quantifiable form in which to pursue commercialization activities. The same rigor and utilization of data-based decision making can yield a deep understanding of the embodiment for which a new invention is most likely to yield commercial opportunity, and, by extension, yield resources by which new fundamental understanding may be pursued.

Early investigators viewed the fields of science and engineering through different lenses.<sup>93</sup> Niels Bohr pursued a furtherance of scientific understanding without much concern as to the commercial implications of his work. Thomas Edison's luminary efforts at not only the lightbulb but a multitude of other engineered devices were built from the viewpoint that commercial success was the best indicator of scientific success. Louis Pasteur struck a keen balance between a search for fundamental understanding and consideration for usage of a new discovery.

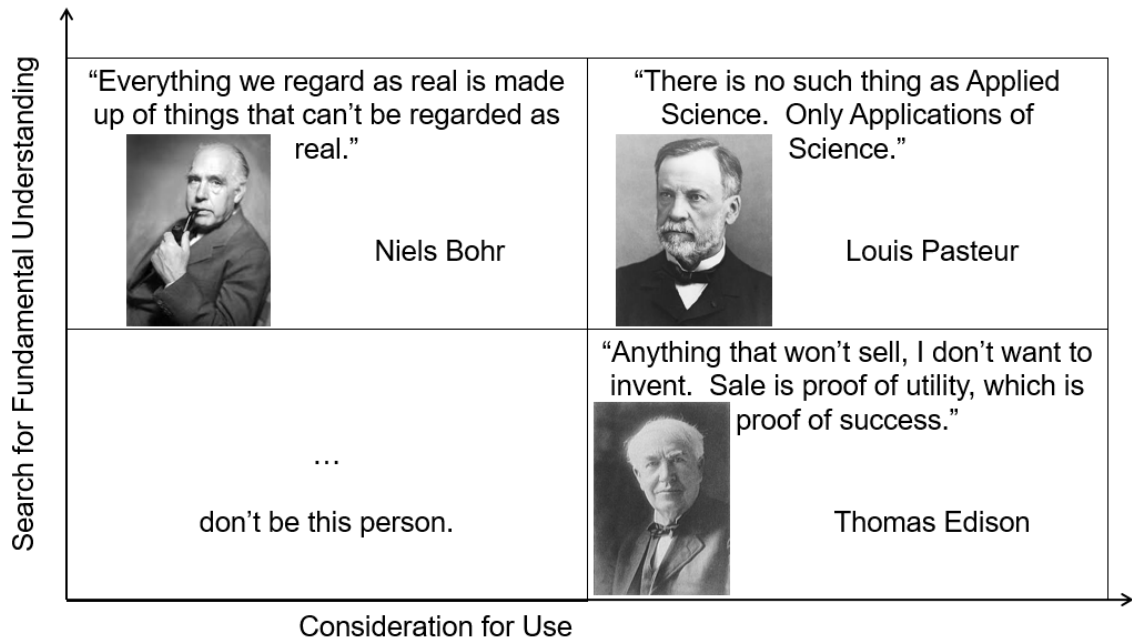


Figure 17: Search for fundamental understanding vs Consideration for use.<sup>94</sup>

The human community finds its greatest furtherance in the unity of diversity as shown by the manners in which these successful and yet inhomogeneous methods produced foundations on which many other discoveries have been erected. It may be that with a robust recognition that evidence-based and objective views such as those practiced by these early pioneers belong throughout the academy, the university will continue to be equipped to foment solutions to the grandest of challenges for centuries to come.

## REFERENCES

- (1) Caruso, F.; Caruso, R. A.; Mohwald, H. Nanoengineering of inorganic and hybrid hollow spheres by colloidal templating. *Science* **1998**, *282*, 1111-1114.
- (2) Alexandre, M.; Dubois, P. Polymer-layered silicate nanocomposites: preparation, properties and uses of a new class of materials. *Materials Science and Engineering: R: Reports* **2000**, *28*, 1-63.
- (3) George, J.; Kumar, R.; Sajeevkumar, V. A.; Ramana, K. V.; Rajamanickam, R.; Abhishek, V.; Nadasabapathy, S.; Siddaramaiah. Hybrid HPMC nanocomposites containing bacterial cellulose nanocrystals and silver nanoparticles. *Carbohydrate Polymers* **2014**, *105*, 285-292.
- (4) Cain, A. A.; Nolen, C. R.; Li, Y.-C.; Davis, R.; Grunlan, J. C. Phosphorous-filled nanobrick wall multilayer thin film eliminates polyurethane melt dripping and reduces heat release associated with fire. *Polymer Degradation and Stability* **2013**, *98*, 2645-2652.
- (5) Hagen, D. A.; Box, C.; Greenlee, S.; Xiang, F.; Regev, O.; Grunlan, J. C. High gas barrier imparted by similarly charged multilayers in nanobrick wall thin films. *RSC Advances* **2014**, *4*, 18354-18359.
- (6) Lan, T.; Pinnavaia, T. J. Clay-Reinforced Epoxy Nanocomposites. *Chemistry of Materials* **1994**, *6*, 2216-2219.
- (7) Baughman, R. H.; Zakhidov, A. A.; de Heer, W. A. Carbon Nanotubes--the Route Toward Applications. *Science* **2002**, *297*, 787-792.

- (8) Ebbesen, T. W.; Ajayan, P. M. Large-scale synthesis of carbon nanotubes. *Nature* **1992**, *358*, 220-222.
- (9) Geim, A. K.; Novoselov, K. S. The rise of graphene. *Nat Mater* **2007**, *6*, 183-191.
- (10) Stankovich, S.; Dikin, D. A.; Dommett, G. H. B.; Kohlhaas, K. M.; Zimney, E. J.; Stach, E. A.; Piner, R. D.; Nguyen, S. T.; Ruoff, R. S. Graphene-based composite materials. *Nature* **2006**, *442*, 282-286.
- (11) Klemm, D.; Kramer, F.; Moritz, S.; Lindström, T.; Ankerfors, M.; Gray, D.; Dorris, A. Nanocelluloses: A New Family of Nature-Based Materials. *Angewandte Chemie International Edition* **2011**, *50*, 5438-5466.
- (12) Gindl, W.; Keckes, J. All-cellulose nanocomposite. *Polymer* **2005**, *46*, 10221-10225.
- (13) Min, Y.; Akbulut, M.; Kristiansen, K.; Golan, Y.; Israelachvili, J. The role of interparticle and external forces in nanoparticle assembly. *Nat Mater* **2008**, *7*, 527-538.
- (14) Moon, R. J.; Martini, A.; Nairn, J.; Simonsen, J.; Youngblood, J. Cellulose nanomaterials review: structure, properties and nanocomposites. *Chem. Soc. Rev.* **2011**, *40*, 3941-3994.
- (15) Habibi, Y.; Lucia, L. A.; Rojas, O. J. Cellulose Nanocrystals: Chemistry, Self-Assembly, and Applications. *Chemical Reviews* **2010**, *110*, 3479-3500.



- (16) Nel, A. E.; Madler, L.; Velegol, D.; Xia, T.; Hoek, E. M. V.; Somasundaran, P.; Klaessig, F.; Castranova, V.; Thompson, M. Understanding biophysicochemical interactions at the nano-bio interface. *Nat Mater* **2009**, *8*, 543-557.
- (17) Brittain, W. J.; Minko, S. A structural definition of polymer brushes. *Journal of Polymer Science Part A: Polymer Chemistry* **2007**, *45*, 3505-3512.
- (18) Kinnane, C.; Such, G.; Caruso, F. Tuning the properties of layer-by-layer assembled poly(acrylic acid) click films and capsules. *Macromolecules* **2011**, *44*, 1194-1202.
- (19) McIlroy, D. A.; Blaiszik, B. J.; Caruso, M. M.; White, S. R.; Moore, J. S.; Sottos, N. R. Microencapsulation of a reactive liquid-phase amine for self-healing epoxy composites. *Macromolecules* **2010**, *43*, 1855-1859.
- (20) Such, G. K.; Tjipto, E.; Postma, A.; Johnston, A. P. R.; Caruso, F. Ultrathin, responsive polymer click capsules. *Nano Letters* **2007**, *7*, 1706-1710.
- (21) Choi, J.; Hore, M. J. A.; Clarke, N.; Winey, K. I.; Composto, R. J. Nanoparticle brush architecture controls polymer diffusion in nanocomposites. *Macromolecules* **2014**, *47*, 2404-2410.
- (22) Jordan, R.; West, N.; Ulman, A.; Chou, Y.-M.; Nuyken, O. Nanocomposites by surface-initiated living cationic polymerization of 2-oxazolines on functionalized gold nanoparticles. *Macromolecules* **2001**, *34*, 1606-1611.
- (23) Haraguchi, K.; Li, H.-J.; Matsuda, K.; Takehisa, T.; Elliott, E. Mechanism of forming organic/inorganic network structures during in-situ free-radical

polymerization in PNIPA–clay nanocomposite hydrogels. *Macromolecules* **2005**, *38*, 3482-3490.

(24) Etxeberria, H.; Tercjak, A.; Mondragon, I.; Eceiza, A.; Kortaberria, G. Electrostatic force microscopy measurements of CdSe-PS nanoparticles and CdSe-PS/poly(styrene-*b*-butadiene-*b*-styrene) nanocomposites. *Colloid Polym Sci* **2014**, *292*, 229-234.

(25) Stuart, M. A. C.; Huck, W. T. S.; Genzer, J.; Muller, M.; Ober, C.; Stamm, M.; Sukhorukov, G. B.; Szleifer, I.; Tsukruk, V. V.; Urban, M.; Winnik, F.; Zauscher, S.; Luzinov, I.; Minko, S. Emerging applications of stimuli-responsive polymer materials. *Nat Mater* **2010**, *9*, 101-113.

(26) Bertrand, O.; Poggi, E.; Gohy, J.-F.; Fustin, C.-A. Functionalized stimuli-responsive nanocages from photocleavable block copolymers. *Macromolecules* **2013**, *47*, 183-190.

(27) Li, D.; Sheng, X.; Zhao, B. Environmentally responsive “Hairy” nanoparticles: Mixed homopolymer brushes on silica nanoparticles synthesized by living radical polymerization techniques. *Journal of the American Chemical Society* **2005**, *127*, 6248-6256.

(28) Hillmyer, M. A.; Lipic, P. M.; Hajduk, D. A.; Almdal, K.; Bates, F. S. Self-assembly and polymerization of epoxy resin-amphiphilic block copolymer nanocomposites. *Journal of the American Chemical Society* **1997**, *119*, 2749-2750.

- (29) Lipic, P. M.; Bates, F. S.; Hillmyer, M. A. Nanostructured thermosets from self-assembled amphiphilic block copolymer/epoxy resin mixtures. *Journal of the American Chemical Society* **1998**, *120*, 8963-8970.
- (30) Liu, J.; Sue, H.-J.; Thompson, Z. J.; Bates, F. S.; Dettloff, M.; Jacob, G.; Verghese, N.; Pham, H. Nanocavitation in self-Assembled amphiphilic block copolymer-modified epoxy. *Macromolecules* **2008**, *41*, 7616-7624.
- (31) Liu, L.; Grunlan, J. C. Clay assisted dispersion of carbon nanotubes in conductive epoxy nanocomposites. *Advanced Functional Materials* **2007**, *17*, 2343-2348.
- (32) Padalkar, S.; Capadona, J. R.; Rowan, S. J.; Weder, C.; Won, Y.-H.; Stanciu, L. A.; Moon, R. J. Natural biopolymers: novel templates for the synthesis of nanostructures. *Langmuir* **2010**, *26*, 8497-8502.
- (33) Eichhorn, S.; Dufresne, A.; Aranguren, M.; Marcovich, N.; Capadona, J.; Rowan, S.; Weder, C.; Thielemans, W.; Roman, M.; Renneckar, S.; Gindl, W.; Veigel, S.; Keckes, J.; Yano, H.; Abe, K.; Nogi, M.; Nakagaito, A.; Mangalam, A.; Simonsen, J.; Benight, A.; Bismarck, A.; Berglund, L.; Peijs, T. Review: current international research into cellulose nanofibres and nanocomposites. *Journal of Materials Science* **2010**, *45*, 1-33.
- (34) Alamri, H.; Low, I. M. Characterization of epoxy hybrid composites filled with cellulose fibers and nano-SiC. *Journal of Applied Polymer Science* **2012**, *126*, E221-E231.
- (35) Cross, L., Schueneman, G., Mintz E. In *Tilte2012*; U.S. Forest Service.

- (36) Pullawan, T.; Wilkinson, A. N.; Eichhorn, S. J. Influence of Magnetic Field Alignment of Cellulose Whiskers on the Mechanics of All-Cellulose Nanocomposites. *Biomacromolecules* **2012**, *13*, 2528-2536.
- (37) Kloser, E.; Gray, D. G. Surface grafting of cellulose nanocrystals with poly(ethylene oxide) in aqueous media. *Langmuir* **2010**, *26*, 13450-13456.
- (38) Elazzouzi-Hafraoui, S.; Nishiyama, Y.; Putaux, J.-L.; Heux, L.; Dubreuil, F.; Rochas, C. The shape and size distribution of crystalline nanoparticles prepared by acid hydrolysis of native cellulose. *Biomacromolecules* **2007**, *9*, 57-65.
- (39) Chandra, R. P.; Gourlay, K.; Kim, C.-S.; Saddler, J. N. Enhancing hemicellulose recovery and the enzymatic hydrolysis of cellulose by adding lignosulfonates during the two-stage steam pretreatment of poplar. *ACS Sustainable Chemistry & Engineering* **2015**.
- (40) Dami, M.; Tatsuo, Y.; Tomoaki, M.; Xiao-Zheng, S. Evaluation of energy consumption and greenhouse gas emissions in preparation of cellulose nanofibers from woody biomass. **2013**, *56*.
- (41) Joshi, S. V.; Drzal, L. T.; Mohanty, A. K.; Arora, S. Are natural fiber composites environmentally superior to glass fiber reinforced composites? *Composites Part A: Applied Science and Manufacturing* **2004**, *35*, 371-376.
- (42) Bledzki, A. K.; Gassan, J. Composites reinforced with cellulose based fibres. *Progress in Polymer Science* **1999**, *24*, 221-274.

- (43) de Figueirêdo, M. C. B.; Rosa, M. d. F.; Ugaya, C. M. L.; Souza Filho, M. d. S. M. d.; Silva Braid, A. C. C. d.; Melo, L. F. L. d. Life cycle assessment of cellulose nanowhiskers. *Journal of Cleaner Production* **2012**, *35*, 130-139.
- (44) Das, S. Life cycle assessment of carbon fiber-reinforced polymer composites. *The International Journal of Life Cycle Assessment* **2011**, *16*, 268-282.
- (45) Khanna, V.; Bakshi, B. R.; Lee, L. J. Carbon nanofiber production. *Journal of Industrial Ecology* **2008**, *12*, 394-410.
- (46) Witter, D. Plastic and Resin Manufacturing in the US. *IBIS World Industry Report* **2015**, 32521.
- (47) Windle, S. Plastic and Resin Manufacturing in the US. *IBIS World Industry Report* **2013**, 32521.
- (48) Mortensen Center for Engineering in Developing Communities. <https://mcedc.colorado.edu/education/graduate-certificate-engineering-developing-communities/courses-even-591929/week-week-fall> (accessed 23 October, 2012).
- (49) Ruiz, B. Car and automobile manufacturing in the US. *IBIS World Industry Report* **2015**, 33611a.
- (50) Ruiz, B. SUV and light truck manufacturing in the US. *IBIS World Industry Report* **2015**, 33611b.
- (51) SCONA TPPP 8112 GA. Instruments, B. A. a., Ed.; Altana Corporation, 2012.
- (52) Trilwax H98. Trillium Specialties LLC, 2014.

- (53) Schatz, C. Two non-covalent methods to decorate nanoparticles with block copolymers. *Macromolecular Chemistry and Physics* **2014**, *215*, 945-957.
- (54) Tang, H.; Butchosa, N.; Zhou, Q. A transparent, hazy, and strong macroscopic ribbon of oriented cellulose nanofibrils bearing poly(ethylene glycol). *Advanced Materials* **2015**, n/a-n/a.
- (55) Peng, B.; Han, X.; Liu, H.; Berry, R. C.; Tam, K. C. Interactions between surfactants and polymer-grafted nanocrystalline cellulose. *Colloids and Surfaces A: Physicochemical and Engineering Aspects* **2013**, *421*, 142-149.
- (56) Araki, J. Electrostatic or steric? - preparations and characterizations of well-dispersed systems containing rod-like nanowhiskers of crystalline polysaccharides. *Soft Matter* **2013**, *9*, 4125-4141.
- (57) Ljungberg, N.; Bonini, C.; Bortolussi, F.; Boisson, C.; Heux, L.; Cavallé, J. Y. New nanocomposite materials reinforced with cellulose whiskers in atactic polypropylene: effect of surface and dispersion characteristics. *Biomacromolecules* **2005**, *6*, 2732-2739.
- (58) Teipel, B. R.; Grunlan, J. Synergy in epoxy nanocomposites with cellulose nanocrystals and boehmite. *Green Materials* **2014**, *2:4*, 222-231
- (59) Tang, L.; Weder, C. Cellulose whisker/epoxy resin nanocomposites. *ACS Applied Materials & Interfaces* **2010**, *2*, 1073-1080.
- (60) Shtein, M.; Nadiv, R.; Lachman, N.; Daniel Wagner, H.; Regev, O. Fracture behavior of nanotube–polymer composites: Insights on surface roughness and failure mechanism. *Composites Science and Technology* **2013**, *87*, 157-163.

- (61) Wang, S.; Zhang, Y.; Ma, X.; Wang, W.; Li, X.; Zhang, Z.; Qian, Y. Hydrothermal route to single crystalline  $\alpha$ -MoO<sub>3</sub> nanobelts and hierarchical structures. *Solid State Communications* **2005**, *136*, 283-287.
- (62) Teixeira, R. F. A.; McKenzie, H. S.; Boyd, A. A.; Bon, S. A. F. Pickering emulsion polymerization using laponite clay as stabilizer to prepare armored “soft” polymer latexes. *Macromolecules* **2011**, *44*, 7415-7422.
- (63) Bon, S. A. F.; Chen, T. Pickering stabilization as a tool in the fabrication of complex nanopatterned silica microcapsules. *Langmuir* **2007**, *23*, 9527-9530.
- (64) Landfester, K.; Fischer, H.; Antonietti, M.; Putlitz, B. Z. The generation of “Armored Latexes” and hollow inorganic shells made of clay sheets by templating cationic miniemulsions and latexes. *Advanced materials* **2001**, *13*, 500-503.
- (65) Xu, S.; Girouard, N.; Schueneman, G.; Shofner, M. L.; Meredith, J. C. Mechanical and thermal properties of waterborne epoxy composites containing cellulose nanocrystals. *Polymer* **2013**, *54*, 6589-6598.
- (66) Bondeson, D.; Oksman, K. Dispersion and characteristics of surfactant modified cellulose whiskers nanocomposites. *Composite Interfaces* **2007**, *14*, 617-630.
- (67) Tzeng, P.; Maupin, C. R.; Grunlan, J. C. Influence of polymer interdiffusion and clay concentration on gas barrier of polyelectrolyte/clay nanobrick wall quadlayer assemblies. *Journal of Membrane Science* **2014**, *452*, 46-53.
- (68) Xu, X.; Liu, F.; Jiang, L.; Zhu, J. Y.; Haagenson, D.; Wiesenborn, D. P. Cellulose nanocrystals vs. cellulose nanofibrils: A comparative study on their

microstructures and effects as polymer reinforcing agents. *Acs Applied Materials & Interfaces* **2013**, *5*, 2999-3009.

(69) Araki, J.; Wada, M.; Kuga, S.; Okano, T. Flow properties of microcrystalline cellulose suspension prepared by acid treatment of native cellulose. *Colloids and Surfaces A: Physicochemical and Engineering Aspects* **1998**, *142*, 75-82.

(70) Beck-Candanedo, S.; Roman, M.; Gray, D. G. Effect of Reaction conditions on the properties and behavior of wood cellulose nanocrystal suspensions. *Biomacromolecules* **2005**, *6*, 1048-1054.

(71) Nelson, K.; Retsina, T. Innovative nanocellulose process breaks the cost barrier. *Tappi Journal* **2014**, *13*, 19-23.

(72) Zhang, Z.; Wu, Q.; Song, K.; Ren, S.; Lei, T.; Zhang, Q. Using cellulose nanocrystals as a sustainable additive to enhance hydrophilicity, mechanical and thermal properties of poly(vinylidene fluoride)/poly(methyl methacrylate) blend. *ACS Sustainable Chemistry & Engineering* **2015**, *3*, 574-582.

(73) Cui, L.; Paul, D. R. Evaluation of amine functionalized polypropylenes as compatibilizers for polypropylene nanocomposites. *Polymer* **2007**, *48*, 1632-1640.

(74) Sathe, S. N.; Rao, G. S. S.; Devi, S. Grafting of maleic anhydride onto polypropylene: Synthesis and characterization. *Journal of Applied Polymer Science* **1994**, *53*, 239-245.

(75) Ehrenstein, G. Overview of selected polymeric materials. *Polymeric Materials, Carl Hanser Verlag, Munich* **2001**, 241.



(76) Iyer, K. A.; Torkelson, J. M. Sustainable green hybrids of polyolefins and lignin yield major improvements in mechanical properties when prepared via solid-state shear pulverization. *ACS Sustainable Chemistry & Engineering* **2015**, 4 (3), 881-889

(77) Kumar, A.; Negi, Y. S.; Choudhary, V.; Bhardwaj, N. K. Effect of modified cellulose nanocrystals on microstructural and mechanical properties of polyvinyl alcohol/ovalbumin biocomposite scaffolds. *Materials Letters* **2014**, 129, 61-64.

(78) Khoshkava, V.; Kamal, M. R. Effect of cellulose nanocrystals (CNC) particle morphology on dispersion and rheological and mechanical properties of polypropylene/CNC nanocomposites. *ACS Applied Materials & Interfaces* **2014**, 6, 8146-8157.

(79) Agarwal, U. P.; Sabo, R.; Reiner, R. S.; Clemons, C. M.; Rudie, A. W. Spatially resolved characterization of cellulose nanocrystal polypropylene composite by confocal raman microscopy. *Applied Spectroscopy* **2012**, 66, 750-756.

(80) *Nanomanufacturing and US Competitiveness - Challenges and Opportunities*; GAO-14-618T. Government Accountability Office, May 20, 2014.

(81) Csere, C., *How automakers will meet 2016 CAFE standards*.  
www.caranddriver.com May 2010

(82) *Industry Report for Automobile Metal Stamping in the US*. IBIS World Report. NAICS 33637. Jun 2012.

(83) Ford engineering material specification: WSS-M4D731-B1  
polypropylene (PP) 20% short glass fiber reinforced, structural, interior.

- (84) *Global markets for nanocomposites, nanoparticles, nanoclays, and nanotubes*. Nano021F. May 2014.
- (85) Automotive News. *Top stories of 2014*.  
<http://www.autonews.com/article/20141229/OEM/312299987/top-stories-of-2014>.  
Accessed July 12, 2014.
- (86) *Plastics and polymer composites in light vehicles*. www.plastics-car.com  
American Chemistry Council. Oct 2015.
- (87) *The global market for composites: Resins, fillers, reinforcements, natural fibers and nanocomposites*: Wellesley, MA2014.
- (88) Charreau, H.; Foresti, M.; Vazquez, A. Nanocellulose patent trends: A comprehensive review on patents on cellulose nanocrystals, microfibrillated and bacterial cellulose. *Recent Patents on Nanotechnology* **2013**, 7, 56-80.
- (89) Hamad, W. Y.; Su, S. NCC-based supramolecular materials for thermoplastic and thermoset polymer composites. International Patent WO 2013/037041A1.
- (90) Gardner, D. J.; Yousoo, H.; Yucheng, P. Method for drying cellulose nanofibrils. United States of America Patent 8,372,320B2.
- (91) Nelson, K.: Phone interview & email conversations. 2015.
- (92) Kumar, S.; Hofmann, M.; Steinmann, B.; Foster, E. J.; Weder, C. Reinforcement of stereolithographic resins for rapid prototyping with cellulose nanocrystals. *ACS Applied Materials & Interfaces* **2012**, 4, 5399-5407.

(93) Hameed, T. *Study of reactions between highly functionalized low molecular weight polyethylne and polyamines to produce thermoset materials*. Thesis. McMaster University. Feb 2012.

(94) Arkilic, E.: Evidence based entrepreneurship. National Science Foundation, 2015.

(95) Prest, C. D.; Browning, L. E.; Pilliod, M. K.; Waniuk, T. A.: Method and apparatus for forming a gold metal matrix composite. US Patent 20,140,361,670, 2014.

(96) Ultrahigh thermal conductivity thermal interface material. In *Flintbox*; March 26, 2015 ed.; Wellspring International: [www.flintbox.com/public/project/27108](http://www.flintbox.com/public/project/27108), 2015.

(97) *Technology Readiness Assessment (TRA)*; Defense, D.o.D: Assistant Secretary of Defense for Research and Engineering, 2011.

APPENDIX: COMMERCIALIZATION OF NEXT-GENERATION  
NANOCOMPOSITES. CASE STUDY OF METAL-MATRIX THERMAL  
INTERFACE MATERIALS

*Description of the problem*

There is an increase in demand for smaller, lighter and more efficient electronic devices to simplify our everyday life, protect the environment, expand global access to education and decrease energy consumption. However, overheating in these devices has been a challenge which has prevented existing technology from meeting key application requirements in this space, and has prevented the necessary improvements in technology for future electronic devices to fully meet the small size, high-power and high-reliability specifications for personal applications (Figure 18).

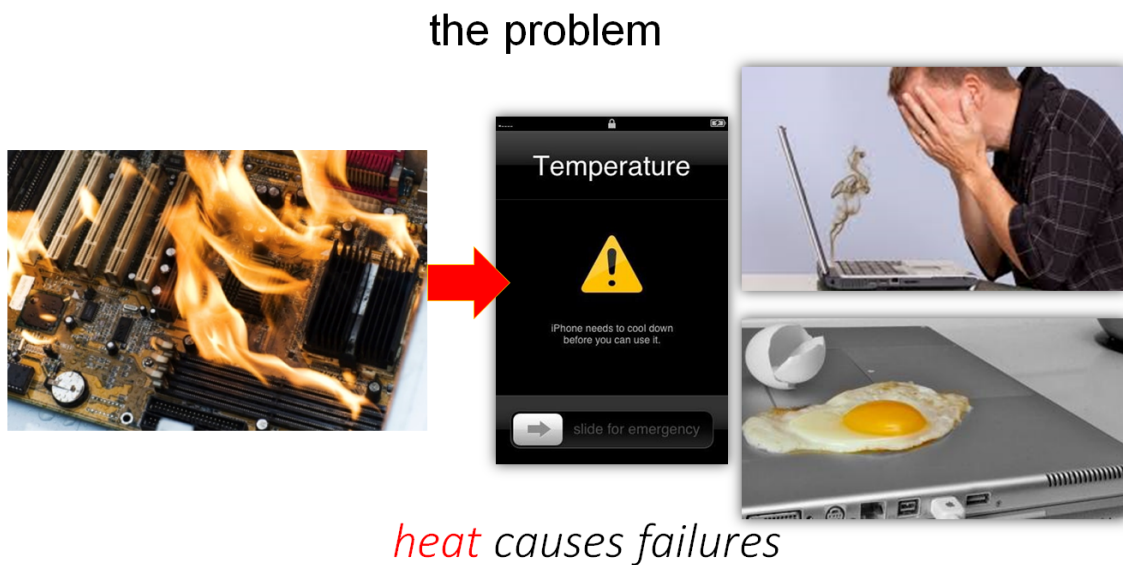


Figure 18: Heat generation occurs in microelectronic and semiconductor devices and can lead to device inoperation and failure.

In some cases, consumer protection groups have advocated discontinuing longer time-scale usage of electronic devices to prevent heat buildup in the device as shown in Figure 19.

## a proposed solution for the end user:



*avoid using your device.*

Figure 19: Users of all types of devices are hindered when thermal mis-management causes device shut down.

As Moore's law has continued to progress, the number of transistors per microchip is now limited by thermal management. Thus, to enable continued improvement in computational capability advancements in thermal management are required. To serve this broad and growing need, Thermal Interface Materials (TIMs)

provide improved contact resistance and conductivity from microprocessors to heat sinks in electronic devices.

The range of materials available to promote device cooling has been largely unchanged for more than a decade and their performance improvements are lagging behind the advances made in electronics applications. A new TIM was developed within the Akbulut Group at Texas A&M University, which can manage heat very effectively and as a result enable electronics to operate faster, more accurately and reliably.

Typical end users for TIMs technology would be electronic device and hardware manufacturers and their suppliers. Industries within which customer discovery interviews are expected to be conducted include device makers for equipment used in personal and supercomputing industries, mobile and telecommunications, military and defense, aerospace and avionics, energy storage (e.g., batteries), healthcare imaging and devices which incorporate wearable technologies. Electronics industries dealing with high-power processors, high-intensity LEDs, vehicle electronics, telecommunication infrastructure, and semiconductor chip packaging can significantly benefit from improvements in TIM technology. The use of batteries in automotive and home-power landscapes is exponentially increasing. Overheating remains a critical issue affecting the safety and limiting the performance of such batteries. Alternative power generation technologies such as wind and solar also rely on robust power storage solutions – all of which will be enhanced by access to next-generation thermal management technology.

*Description of the proposed solution*

Principle aspects of the current technology center on the unique approach for achieving high-capacity, uniform dissipative cooling. TIMs are needed because of mismatching surfaces between the microprocessor and the heat sink as shown in Figure 20. At the micron scale, these surfaces barely touch, trapping air between them which leads to poor conductivity and uneven cooling. Therefore, an interface material which is both highly conductive and compliant enough to fill the voids between the surfaces is needed.

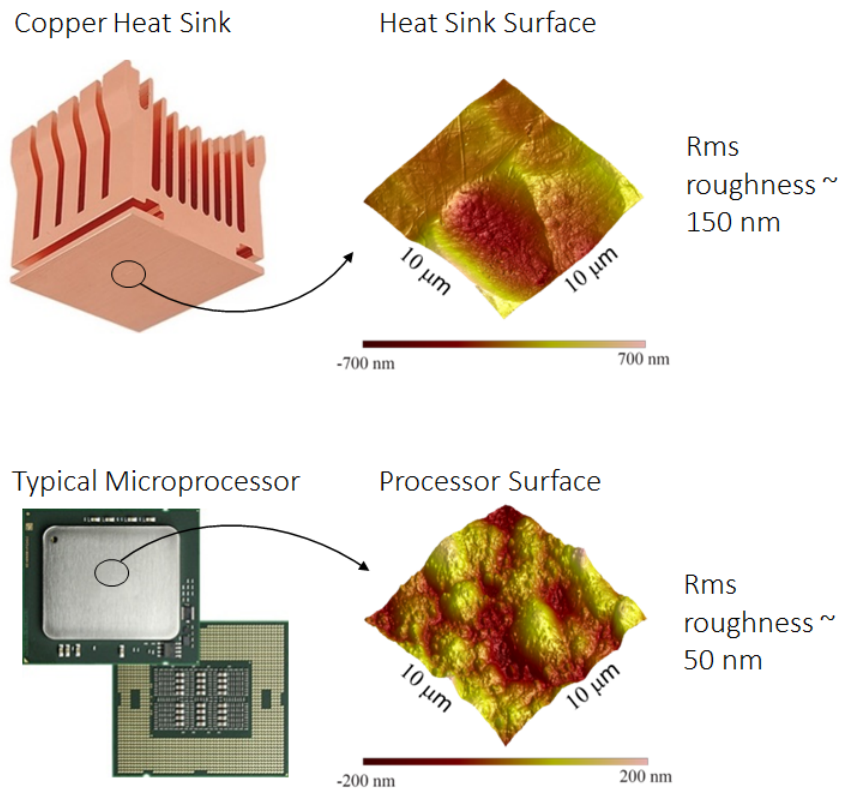


Figure 20: Surface mismatch between thermal source and heat sink (Atomic Force Microscopy (AFM) surface contour shown).

An ideal TIM would be softer than the usually metallic microprocessor packaging and heat-sink surfaces yet would offer similar conductivity as these metallic components. Figure 21 illustrates the challenges posed when hard yet conductive TIMs are utilized for dissipative cooling.

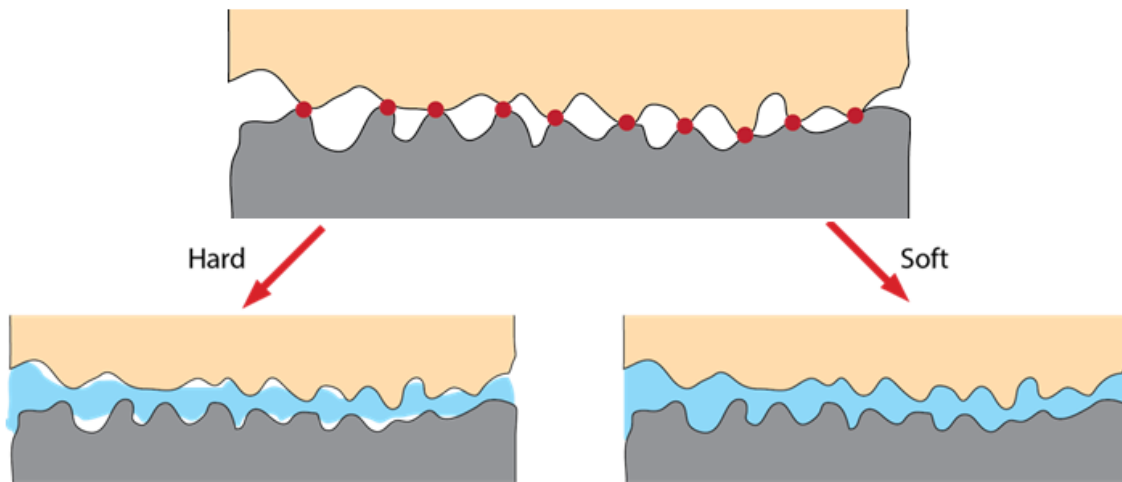


Figure 21: Poor surface-surface contact leads to poor thermal conductivity.

The inspiration for this technology came from NSF Award # 1236532, which helped obtain a fundamental understanding of the interactions and adsorption of nanoparticles on solids surfaces as well as control the kinetics and thermodynamics of nanoparticulate (BN nanosheets) adsorption on solid (copper) surfaces. The approach for this technology is based on the deposition of BN nanosheets onto copper surfaces as copper continuously grows electrochemically. The developed hybrid material significantly outperforms the current-state-art of TIMs (Figure 23).



Based on this fundamental understanding, a novel TIM technology was developed, which involves a nanocomposite material loaded with nanoparticles (Boron Nitride (BN) nanosheets). The formation of this nanocomposite requires the adsorption of BN nanosheets on solid metallic surfaces. The resultant thin film is uniform, flexible, compliant and robust (Figure 24).

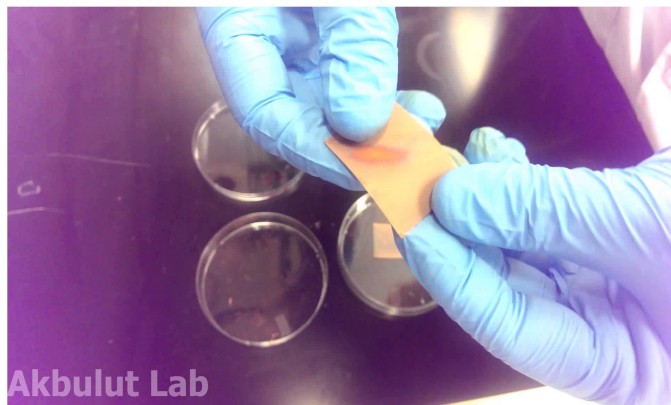


Figure 22: Next generation Thermal Interface Materials

The effective thermal conductivity of many commercially available TIMs are on the order of 5–10 W/(m·K), which is considerably lower than the thermal conductivities of typical mating components. The best current technology has conductivity values which range from 20 – 80 W/(m·K) as shown in Figure 23.

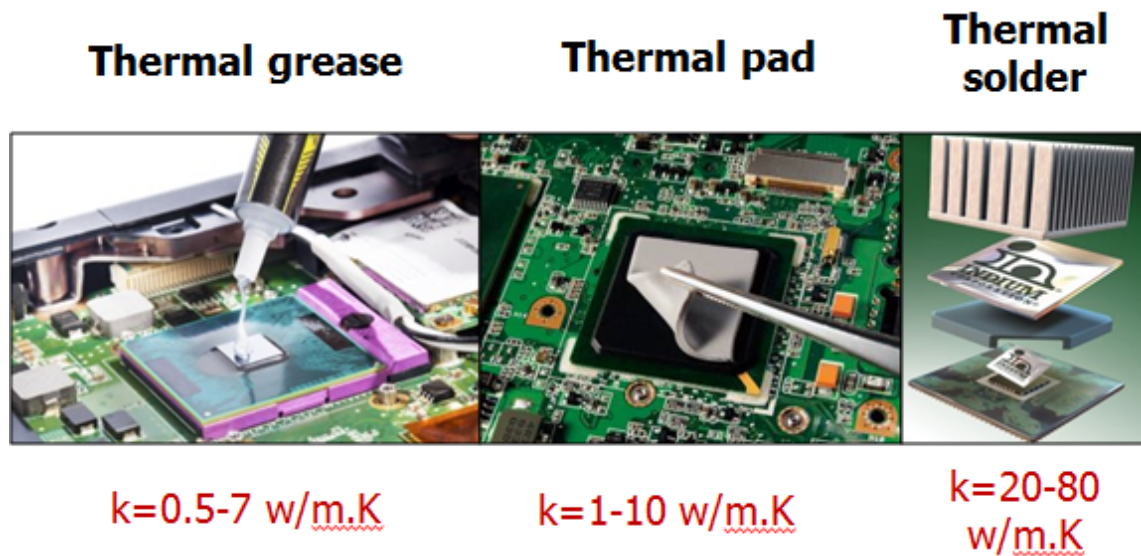


Figure 23: Current Generation Thermal Interface Materials with corresponding thermal conductivities

The novel TIM solution developed utilizes a ceramic nanoparticle functionalized with soft ligands, which is then electrocodeposited in a metal matrix. This is all achieved by a TIM produced in an easy three step process (Figure 24). The developed approach is highly scalable as it primarily relies on a reaction tank and a pulsating DC power source, thereby making it likely to be commercially cost-effective. This technology therefore provides a nanocomposite which is a combination of metallic, ceramic and polymeric microstructures. For these reasons, primarily, it seems likely that this technology may be a good fit for commercialization.

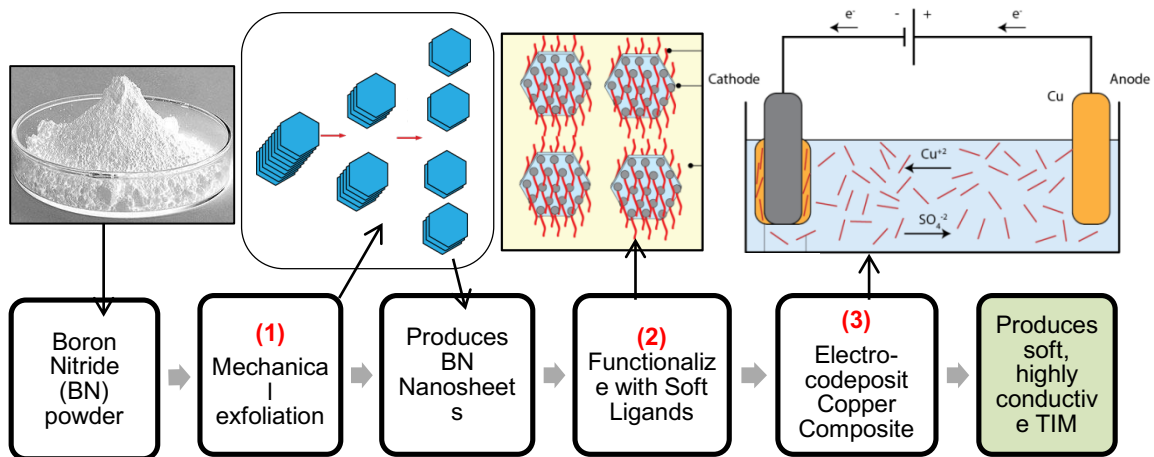


Figure 24: Three step process to produce next-generation TIMs

The new material has ultra-high thermal conductivity much greater than 250 W/(m·K) (Figure 25). In addition to this outstanding conductivity, it has high compliance, flexibility, and compatibility with metals, and achieves a total bulk thermal impedance of  $1-4 \times 10^{-3} \text{ K} \cdot \text{cm}^2/\text{W}$  which is an order of magnitude lower than commercially available TIMs. To date, proof-of-concept experiments have yielded measurable decreases in component-cooling times.

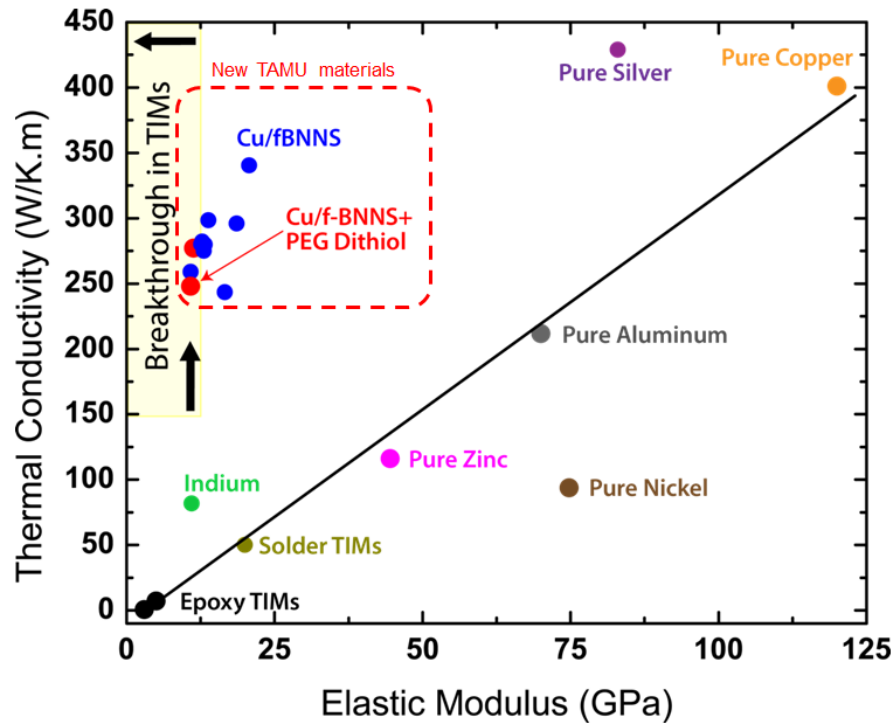


Figure 25: Breakthrough TIMs must exhibit low elastic modulus and high thermal conductivity

Next generation TIMs are composed of innovations in the filled-polymer, metal-matrix composite, and solder categories. There is significant interest in capitalizing on the transport-properties of metallic materials, hence metal-matrix composites are a promising pathway to achieve needed system gains. The challenges to this solution path are found in the mechanical properties of the material: mechanical and transport properties are due in large part to the electron structure and hence are intrinsic values of metals themselves. It is thus difficult to alter one whereas maintaining the other. This is why the current technology is so interesting. The conductivity (transport property) is barely reduced (38% reduction from 400 W/m·K in pure copper to >250 W/m·K in the

invention) whereas the stiffness is reduced by 88% (125 GPa in pure copper to 15 GPa in the invention) (Figure 25).

### *Development plan*

As TIMs technology is still early stage, it must be developed to cross the “Valley of Death” as shown in Figure 26. An appropriate development plan is therefore necessary and is presented.

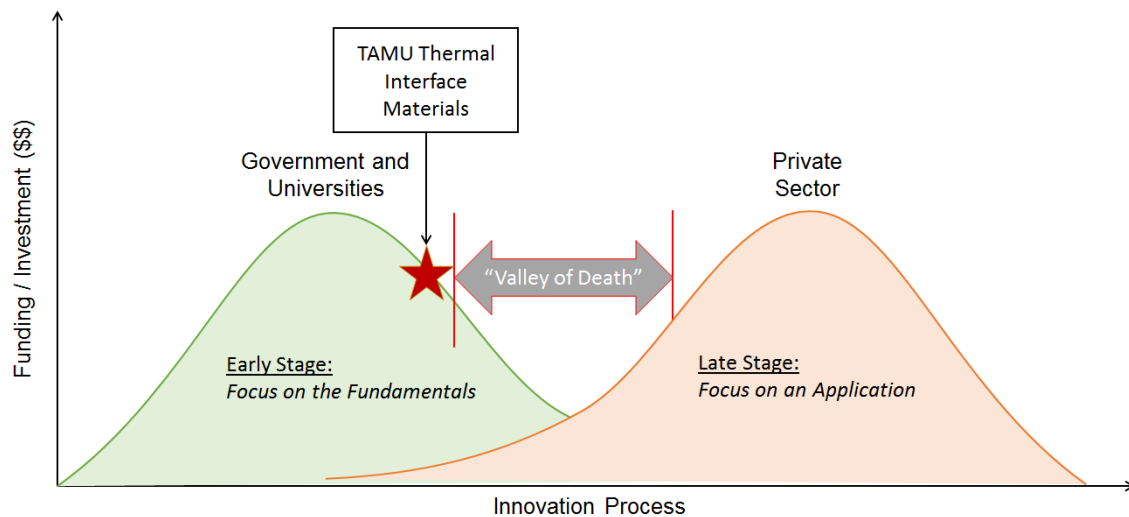


Figure 26: Innovation stage: next generation Thermal Interface Materials

### **Risks**

The technology is risky from an economic standpoint. There will be significant barriers to entry into new markets, such as:

1. Institutional inertia (customer’s resistance to change)
2. Unknown technology (this will be disruptive to old technology)

3. Management change (customers with whom we begin discussions may not stay through project)
4. New value chain (existing manufacturers may not be able to support the processes)
5. Scale-up timeline (unknown)
6. Manufacturing readiness (TBD. Between MRL-2 – 4)
7. Final material configuration (unknown)
8. Economics (unknown)
9. Competing intellectual property (full field unknown. At least one recent patent filed by Apple is very close)<sup>94</sup>

### **Technology/Manufacturing Readiness Level (TRL / MRL)**

Online references to this technology score it at Technology Readiness Level 6 (TRL-6) (Table 6).<sup>95</sup> However, the component must be scaled prior to becoming a full system-level prototype. Therefore, it is likely that this technology is at TRL-5.<sup>96</sup> There is significant development time, and subsequent de-risking, between TRL-5 and TRL-6. The material is between Manufacturing Readiness Level 2 (MRL-2) and (MRL) four (4) using the Department of Defense (DoD) scale (Table 7).<sup>97</sup> Thus, the TRL and MRL must be brought into congruency, which is a principle function of an early stage venture in this effort.

The main reasons for the assessed TRL and MRL are:

1. The TIMs are not scaled to sheet- or roll-sizes (anything beyond postage-stamp size)

2. There have been, at various points during development, difficulties obtaining uniform nanoparticle diffusion. The robustness of the present uniformity solution needs to be further understood to ensure it will scale well to sheet, roll or a device itself
3. The TIMs used in video, etc., are in a miniature sheet-form which is not fastened to any other component by way of adhesive, mechanical or threaded fastener. In final assembly environments, it will be critical to ensure the TIMs will remain in place on the electronic device, once put in place

Further, additional investigation is warranted, and will be conducted as a function of normal scale-up research, as to why a >230% improvement in thermal conductivity (>250 W/m·K vs 75 W/m·K for indium (Figure 25)) translates only to a 37% improvement in cooling time for the same setup (4.63 vs 7.34 min). As the invention is still in its infancy such system cooling performance can be readily improved. But the technology is not without risk and may never be able to be sold at price points that customers are willing to make a change, to adopt.

Table 6 - Technology Readiness Level Pertinent Position (selection from full DoD TRL)

<b>Technology readiness level</b>	<b>Description</b>	<b>Supporting information</b>
4. Component and/or breadboard validation in laboratory environment	Basic technological components are integrated to establish that they will work together. This is relatively “low fidelity” compared with the eventual system. Examples include integration of “ad hoc” hardware in the laboratory.	System concepts that have been considered and results from testing laboratory-scale breadboard(s). References to who did this work and when. Provide an estimate of how breadboard hardware and test results differ from the expected system goals.
5. Component and/or breadboard validation in relevant environment	Fidelity of breadboard technology increases significantly. The basic technological components are integrated with reasonably realistic supporting elements so they can be tested in a simulated environment. Examples include “high-fidelity” laboratory integration of components.	Results from testing laboratory breadboard system are integrated with other supporting elements in a simulated operational environment. How does the “relevant environment” differ from the expected operational environment? How do the test results compare with expectations? What problems, if any, were encountered? Was the breadboard system refined to more nearly match the expected system goals?
6. System/subsystem model or prototype demonstration in a relevant environment	Representative model or prototype system, which is well beyond that of TRL-5, is tested in a relevant environment. Represents a major step up in a technology’s demonstrated readiness. Examples include testing a prototype in a high-fidelity laboratory environment or in a simulated operational environment.	Results from laboratory testing of a prototype system that is near the desired configuration in terms of performance, weight, and volume. How did the test environment differ from the operational environment? Who performed the tests? How did the test compare with expectations? What problems, if any, were encountered? What are/were the plans, options, or actions to resolve problems before moving to the next level?



Table 6 Continued

<b>Technology readiness level</b>	<b>Description</b>	<b>Supporting information</b>
7. System prototype demonstration in an operational environment.	Prototype near or at planned operational system. Represents a major step up from TRL-6 by requiring demonstration of an actual system prototype in an operational environment (e.g., in an aircraft, in a vehicle, or in space).	Results from testing a prototype system in an operational environment. Who performed the tests? How did the test compare with expectations? What problems, if any, were encountered? What are/were the plans, options, or actions to resolve problems before moving to the next level?

Table 7 - Manufacturing Readiness Level with TIMs position highlighted (selection from full DoD MRL)

<b>Phase (as specified by DoD I 5000.02<sup>[7]</sup>)</b>	<b>Leading to</b>	<b>Definition</b>	<b>Description</b>
Material Solutions Analysis	Material Development Decision review	Basic manufacturing implications identified	Basic research expands scientific principles that may have manufacturing implications. The focus is on a high level assessment of manufacturing opportunities. The research is unfettered.
		Manufacturing concepts identified	Invention begins. Manufacturing science and/or concept described in application context. Identification of material and process approaches are limited to paper studies and analysis. Initial manufacturing feasibility and issues are emerging.
		Manufacturing proof of concept developed	Conduct analytical or laboratory experiments to validate paper studies. Experimental hardware or processes have been created, but are not yet integrated or representative. Materials and/or processes have been characterized for manufacturability and availability but further evaluation and demonstration is required.
	Milestone A decision	Capability to produce the technology in a laboratory environment.	Required investments, such as manufacturing technology development identified. Processes to ensure manufacturability, producibility and quality are in place and are sufficient to produce technology demonstrators. Manufacturing risks identified for prototype build. Manufacturing cost drivers identified. Producibility assessments of design concepts have been completed. Key design performance parameters identified. Special needs identified for tooling, facilities, material handling and skills.

In order to assess the market readiness of this technology, and in order to determine appropriate customers for the technology, participation in the National Science Foundation Innovation-Corps (I-Corps) program was instituted.

### **Customer discovery**

It is necessary to gain voice of the market data (VoM) during I-Corps interviews and other market research activities conducted during the program. Given the stratified nature of the supply chain for electronic and microprocessor devices it is necessary to map the supplier base and raw material manufacturers. Candidate interviewees include engineers at Apple, Intel, and Tesla Motors as these are examples of typical end-use customers. Interviews within the supply base will also be beneficial. These customers and others have needs to cool microprocessors, high-frequency electronics, and lithium-ion batteries through a heat sink coupled with TIMs. For these applications, the thermal conductivity of TIMs sets the limit of cooling and energy efficiency. As electronic components get smaller and high energy efficiency is pushed for Green computing, these industries are increasingly needing new TIMs with thermal conductivities much greater than  $10 \text{ W}/(\text{m}\cdot\text{K})$ .

This TIMs technology has already been demonstrated at the proof-of-concept stage and is now at the initial prototype stage. Its development is ripe for input from the VoM. This VoM data will enable us to select the pathway to our minimum viable product(s).

It is anticipated that through participation in the I-Corps program and especially the intensive interview process, the technology will move from its Early-Stage position to

one which is nearer to Market Ready. Initial scale up activities, optimization of cooling performance by manipulation of processing parameters and minimization of chemical use will all then be subsequently initiated. A pressing question we seek to answer will be whether to pursue funding to fully scale and commercialize the technology ourselves or to seek to license the technology to elsewhere in the supply base.

To conduct adequate customer discovery it is necessary to get out of the building to gain the broadest perspective possible (see Figure 27). Given this technology started in College Station, TX, there was significant travel required to gain perspective from industrial users.

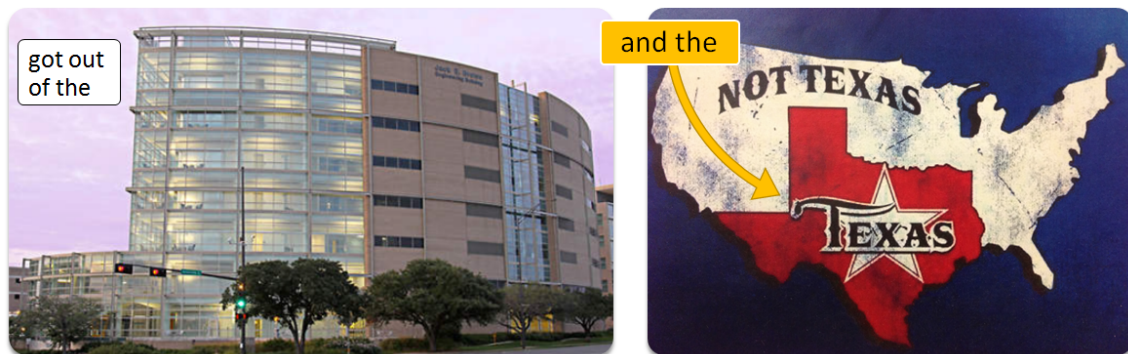


Figure 27: The National Science Foundation I-Corps Program mandates customer discovery away from users who may be familiar with a technology under investigation.

A typical customer archetype for this technology is a hardware engineer with design control over various types of electronic assemblies. Figure 28 illustrates a typical customer archetype for this technology and associated end-use applications. It is of critical import to discern the appropriate customer for any type of new technology.

Engineers, scientists, and academicians often fall prey to the notion that an excellent solution is a sufficient condition to generate market acceptance, and, eventually, revenue from product or technology sales. Technical efficacy is a necessary but insufficient condition to produce product sales. A robust understanding of the commercial market is required to generate commercial opportunity and business growth.

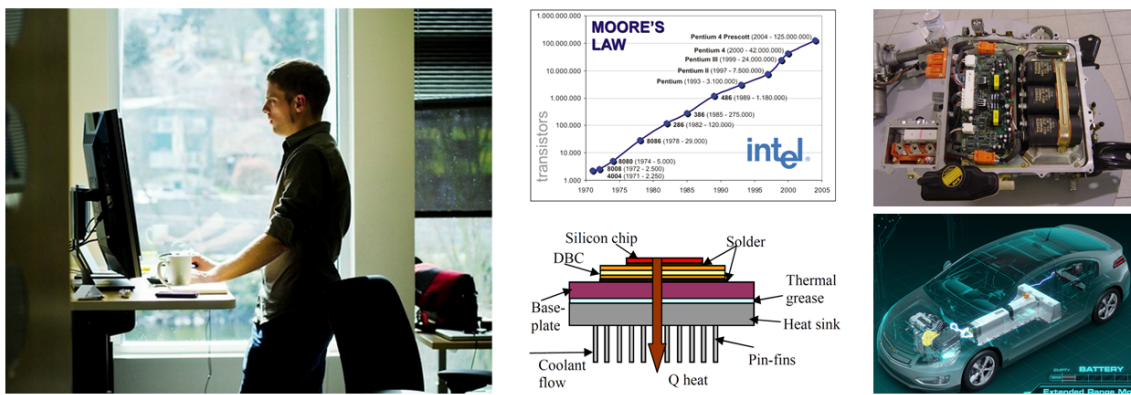


Figure 28: typical customer archetype, a typical customer constraint (Moore’s Law) and example end-use applications for TIMs

Once a customer archetype is defined and example applications are known, examination of existing business in the space is required.

**Known suppliers of current TIMs solutions**

There are myriad companies operating in this space both in the direct supply and technology roles.

*Key Vendors*

- Cookson Electronics Assembly Materials
- Dow Corning

- Henkel
- Honeywell International
- Laird
- Zalman Tech

*Other Prominent Vendors*

- 3M
- Arctic Silver
- Indium
- NuSil Technology
- Seal King Industrial
- Stockwell Elastomerics
- Thermal Transfer Composites
- Universal Science
- Vanguard products

*Risk mitigation plan*

A candidate company would adopt these initial steps to develop and therefore de-risk, the technology:

1. Initiate a rigorous market-study via participation in the NSF I-Corps program
  - a. This program is funded via the National Science Foundation to a secondary education institution such as TAMU with support for a graduate student, and all program expenses including travel.

- b. This six-month program is front-loaded into seven weeks of intensive interviews and information gathering from experts/agents in the Thermal Materials space. The key deliverables are significant industry relationships and a Go/No Go decision on commercialization of the technology as-is.
2. Instead of I-Corps, (if program participation is not possible) a candidate company would need to initiate market development activities with key experts/agents in this space
3. Grant proposals providing funds to commercially develop this material are available. Potential sources include:
  - a. National Science Foundation via SBIR funding pathway
  - b. Department of Defense
  - c. Commercial organizations within defense, electronics and automotive industries

#### *Timeline and milestones*

The development of TIMs is intended to provide exposure to the commercial market for this material, in conjunction with the provision/invention of scale-up technology. The development path could follow a NSF pathway via established and trusted SBIR program phases. Figure 29 illustrates the projected development timeline with milestones indicated (e.g., X's and the Hiring Markers).

		TIMs Market Development Timeline																											
Year		2015				2016				2017				2018				2019				2020							
Quarter		Q1	Q2	Q3	Q4	Q1	Q2	Q3	Q4	Q1	Q2	Q3	Q4	Q1	Q2	Q3	Q4	Q1	Q2	Q3	Q4	Q1	Q2	Q3	Q4				
<b>TIMs Product Development</b>		[Green shaded]																											
<b>Market Development</b>		[Green shaded]																											
NSF iCorps or similar		\$50k (6 mos)																											
7-week intensive portion		[Green shaded]																											
Final Report						X																							
<b>Early Stage Developmental Funding</b>																													
SBIR Ph1 or similar						+1 FTE				\$150k																			
Proposal due date						X																							
Notification of funding						X																							
Final Report										X																			
<b>Ph 2 Program</b>																													
Proposal due date										X				+1 FTE				Ph2: \$750k (24 mos)				Ph2b: \$500k (18 mos)							
Notification of funding										X																			
Reports														X				X				X				X			
<b>Large Capital Raise</b>																													
Round 1: \$1.0MM (Outside Funds)																		[Green shaded]											
Round 2: \$5.0MM (Outside Funds)																						[Green shaded]							
Round 3: \$10.0MM (Outside Funds)																						+1 FTE							
<b>First Revenue</b>																													
From TIMs																		[Green shaded]				[Green shaded]							

Figure 29: TIMs development timeline and milestones.

This timeline hinges upon:

1. the raise of approximately half of the total required funds raised via NSF or similar organization or, if a more accessible funding path is identified, a greater amount of funds will be raised more rapidly
2. the ability to add technical headcount at the appropriate times (e.g., when new funds equaling approximately half of the total cost to support a new FTE are appropriated/promised, a decision to initiate a new hire can be made)
3. the market analysis providing a Go decision whereby the demanded specifications can be supplied at a profitable price point



It should be noted that a candidate company would need to supply approximately half of all required investment from internal funding or other sources. Any external development funding awarded should be viewed as a catalyst for market entry, not the sole enabler. Additionally, it is believed that if additional funding becomes available during the development timeline, additional headcount may be procured which will directly serve to speed the project.

*Description of the potential commercial impact*

The global market for this technology is expected to grow to \$962.0 million by 2020 with thermal management hardware (fans and blowers, heat sinks) accounting for 84% of this growth. Commercial pricing for current generation TIM technology varies widely by material capability and industry served. For instance, graphite-based TIMs cost \$50–100 per square meter whereas silica filled elastomer TIMs cost \$5–20 per square meter. Given that our solution improves thermal performance about 3-fold in comparison to the best available TIMs, we anticipate that a customer would pay at least \$100/m<sup>2</sup> of our TIM.

*Results from the National Science Foundation I-Corps program*

Over a seven week period, 104 customer discovery interviews were conducted. Of these, 93 were conducted in person. Interviews were conducted in the following cities:

1. California
  - a. San Jose
  - b. Santa Clara

- c. San Francisco
  - d. Palo Alto
- 2. Texas
  - a. College Station
  - b. Houston
  - c. Austin
  - d. Richardson
  - e. Red Oak
- 3. Massachusetts
  - a. Boston
- 4. Arizona
  - a. Phoenix
  - b. Chandler
- 5. Michigan
  - a. Detroit
  - b. Ann Arbor
- 6. Virginia
  - a. Arlington
- 7. The District of Columbia

Figure 30 shows a selection of the companies visited during these interviews.

The interviews were conducted by one or two members of the I-Corps team, usually the Entrepreneurial Lead and the Industry Mentor. Typical interviewees included members

of the technical community for the company or organization under consideration. These interviewees were most often considered as end-users of the technology (Figure 28).

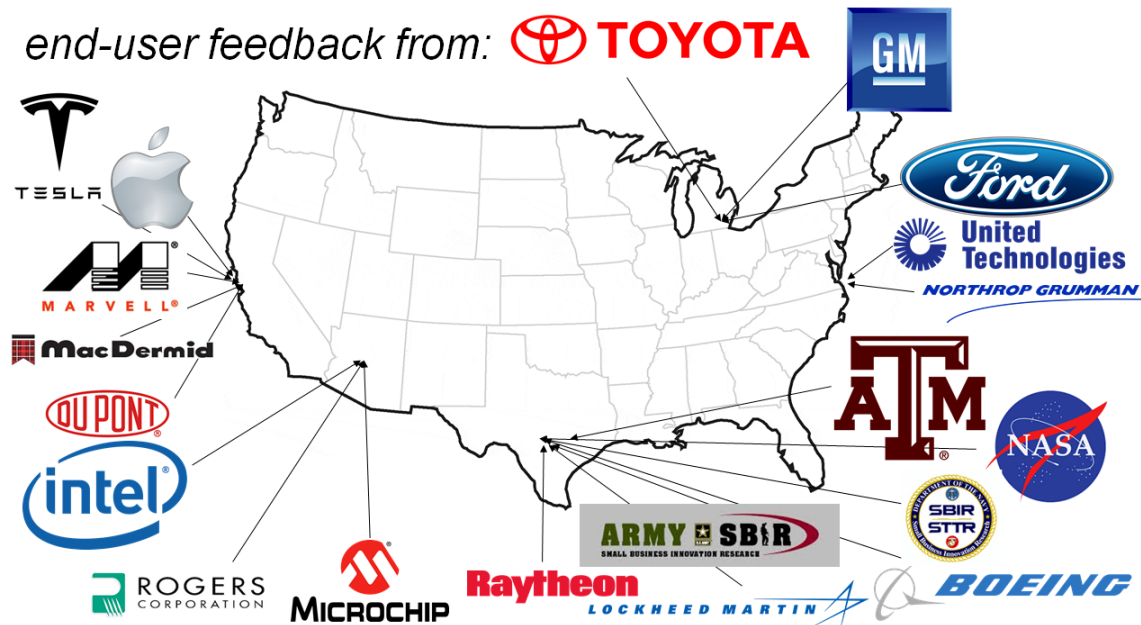


Figure 30: End-user feedback was gained from technical groups across the United States.

Example end user feedback was compiled through the interview portion of the I-Corps program. General respondent feedback was highly positive as to the value propositions of the technology within the customer segments queried. Thought leaders and influencers in the microelectronic, computer component and Li-battery communities issued responses to the technology queries shown in Figure 31.

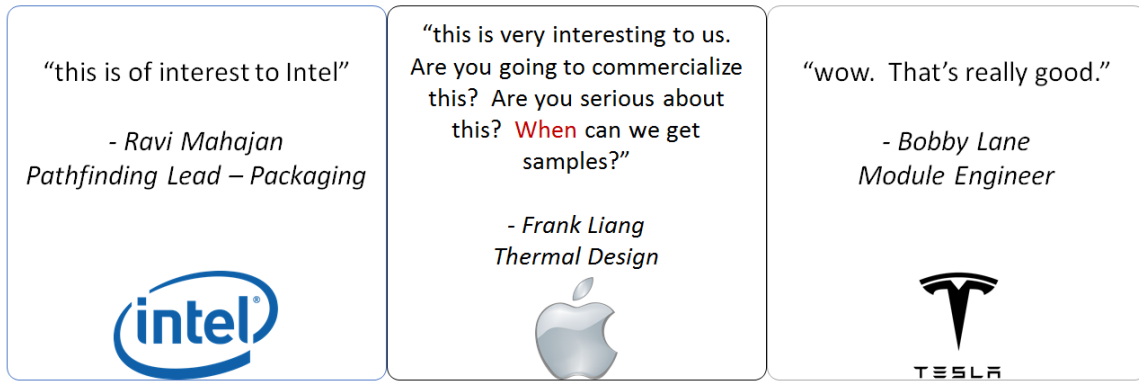


Figure 31: Feedback from selected End Users.

### *Conclusions: Thermal Interface Materials*

This method for fabricating hybrid metal-matrix ceramic-ligand nanocomposites provides a simple two-step method for preparation of materials with 300% better performance than their closest known competition. The results of the I-Corps program were highly positive with regard to the fitment of the technology to provide improved dissipative cooling for multiple customer segments across the electronic device industrial ecosystem. The TIMs technology in question is still quite early in development, however, and not yet ready for commercialization as compared to the CN-polymer nanocomposites of Chapter II and Chapter III.

Future work for the TIMs technology includes:

1. Cost analysis and pricing model development
2. Manufacturing scale-up analysis to be performed
3. Sales Channel development

4. Conduct additional customer interviews. 400–500 interviews represent an actual number required to fully survey an unknown market.